

AD-A053 389

KAMAN AVIDYNE BURLINGTON MASS

F/6 1/3

ANALYTICAL PREDICTIONS AND CORRELATION WITH EXPERIMENTS FOR THE--ETC(U)

JUL 77 R P YEGHIAYAN

DNA001-75-C-0179

UNCLASSIFIED

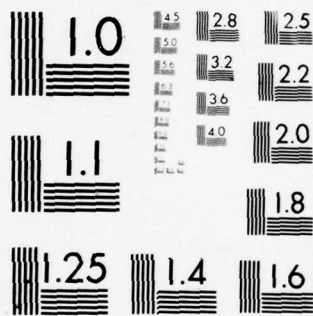
KA-TR-142

DNA-4446F

NL

1 OF
AD
A053389





MICROCOPY RESOLUTION TEST CHART
NATIONAL BUREAU OF STANDARDS-1963-A

AD A 053389

12

AD-E 300 171

DNA 4446F

ANALYTICAL PREDICTIONS AND CORRELATION WITH EXPERIMENTS FOR THERMAL/BLAST EXPOSURE OF AIRCRAFT PANELS

Kaman AviDyne

Division of Kaman Sciences Corporation

83 Second Avenue

Burlington, Massachusetts 01803

July 1977

Final Report for Period 15 December 1975—30 September 1976

CONTRACT No. DNA 001-75-C-0179

APPROVED FOR PUBLIC RELEASE;
DISTRIBUTION UNLIMITED.

THIS WORK SPONSORED BY THE DEFENSE NUCLEAR AGENCY
UNDER RDT&E RMSS CODE B342076464 N99QAXAE51021 H2590D.

Prepared for

Director

DEFENSE NUCLEAR AGENCY

Washington, D. C. 20305



AU NO. _____
DDG FILE COPY

1

Destroy this report when it is no longer
needed. Do not return to sender.



AD NUMBER

E300171

FIELD 2: FLD/GRP(S)
FIELD 3: ENTRY CLASS
FIELD 4: NTIS PRICES
FIELD 5: SOURCE NAME
FIELD 6: UNCLASS. TITLE

FIELD 7: CLASS. TITLE
FIELD 8: TITLE CLASS.
FIELD 9: DESCRIPTIVE NOTE
FIELD 10: PERSONAL AUTHORS
FIELD 11: REPORT DATE
FIELD 12: PAGINATION
FIELD 13: SOURCE ACRONYM
FIELD 14: REPORT NUMBER
FIELD 15: CONTRACT NUMBER
FIELD 16: PROJECT NUMBER
FIELD 17: TASK NUMBER
FIELD 18: MONITOR SOURCE
FIELD 19: MONITOR SERIES
FIELD 20: REPORT CLASS
FIELD 21: SUPPLEMENTARY NOTE
FIELD 22: ALPHA LIMITATIONS

FIELD 23: DESCRIPTORS
FIELD 24: DESCRIPTOR CLASS.
FIELD 25: IDENTIFIERS

FIELD 26: IDENTIFIER CLASS.
FIELD 27: ABSTRACT

FIELD 28: ABSTRACT CLASS.
FIELD 29: INITIAL INVENTORY

FIELD 30: ANNOTATION
FIELD 31: SPECIAL INDICATOR
FIELD 32: REGRADING CATEGORY
FIELD 33: LIMITATION CODES
FIELD 34: SOURCE SERIAL
FIELD 35: SOURCE CODE
FIELD 36: DOCUMENT LOCATION
FIELD 37: CLASSIFIED BY
FIELD 38: DECLASSIFIED ON
FIELD 39: DOWNGRADED TO CONF.
FIELD 40: GEOPOLITICAL CODE
FIELD 41: SOURCE TYPE CODE
FIELD 42: TAB ISSUE NUMBER

01030 13130

U

HC MF
KAMAN AVIDYNE BURLINGTON MASS
ANALYTICAL PREDICTIONS AND CORRE
EXPOSURE OF AIRCRAFT PANELS.

U

FINAL REPT. 15 DEC 75 - 30 SEP 7
YEGHIAYAN, RAFFI P. ;

JUL 77

78P

KA-TR-142

DNA001-75-C-0179

N99QAXA

E510

DNA

4446F

U

DISTRIBUTION OF DOCUMENT CONTROL
20305. THIS DOCUMENT IS NOT AVAIL
BY DEFENSE NUCLEAR AGENCY, WASHIN

•STRUCTURAL ANALYSIS, OVERPRESSUR
U

•AIRCRAFT STRUCTURES, THERMAL TES
EFFECTS(AEROSPACE), BLAST TESTS,

STRUCTURAL DYNAMICS, WU21

U

A STUDY OF THE EFFECTS OF THERMAL
CARRIED OUT JOINTLY BY KAMAN AVID
CENTER. PRE-TEST PLANNING AND ANA
AVIDYNE EMPLOYING THE DNA 2048 ME
RESULTS OBTAINED AT NSWC. CORRELA
INDIVIDUAL EFFECTS OF INTERNAL PR
CORRELATION PROVED TO BE A DIFFIC
WHICH HAVE A LOW CONFIDENCE LEVEL

U

0

0

1 21

F

194970

7

2507

4

00--00

30

MF

ADYNE BURLINGTON MASS

ANAL PREDICTIONS AND CORRELATION WITH EXPERIMENTS FOR THERMAL/BLAST
OF AIRCRAFT PANELS.

PERIOD: 15 DEC 75 - 30 SEP 76,
RAFFI P. 1

5-C-0179

THIS DOCUMENT IS NOT AVAILABLE FROM DDC. CATALOGING INFORMATION SUPPLIED
BY THE NUCLEAR AGENCY, WASHINGTON, DC 20305.

ANALYSIS, OVERPRESSURE

Response
STRUCTURES, THERMAL TESTS, TEMPERATURE MEASUREMENTS, BLAST
(AEROSPACE), BLAST TESTS, RADIATION EFFECTS (AEROSPACE),
DYNAMICS, WU21

THE EFFECTS OF THERMAL/BLAST EXPOSURE ON REPRESENTATIVE AIRCRAFT PANELS WAS
STUDIED JOINTLY BY KAMAN AVIDYNE AND THE NAVAL SURFACE WEAPONS
CENTER. PRE-TEST PLANNING AND ANALYTIC PREDICTIONS WERE CARRIED OUT AT KAMAN
EMPLOYING THE DNA 2048 METHODS, AND WERE COMPARED WITH THE EXPERIMENTAL
RESULTS OBTAINED AT NSWC. CORRELATION WITH EXPERIMENTAL RESULTS WAS GOOD FOR THE
EFFECTS OF INTERNAL PRESSURIZATION OR BLAST OVERPRESSURE ON PANELS, BUT
IT WAS PROVED TO BE A DIFFICULT TASK FOR EXPERIMENTS INVOLVING THERMAL EXPOSURE,
AT A LOW CONFIDENCE LEVEL.

(18) DNA, SBIE (19) 4446F, AD-E300 171

UNCLASSIFIED

SECURITY CLASSIFICATION OF THIS PAGE (When Data Entered)

REPORT DOCUMENTATION PAGE		READ INSTRUCTIONS BEFORE COMPLETING FORM
1. REPORT NUMBER DNA 4446F	2. GOVT ACCESSION NO.	3. RECIPIENT'S CATALOG NUMBER
4. TITLE (and Subtitle) ANALYTICAL PREDICTIONS AND CORRELATION WITH EXPERIMENTS FOR THERMAL/BLAST EXPOSURE OF AIRCRAFT PANELS	5. AUTHOR(s) Raffi P. Yeghiayan	6. TYPE OF REPORT & PERIOD COVERED Final Report. Unpublished 15 Dec 75—30 Sep 76
7. AUTHOR(s)	8. CONTRACT OR GRANT NUMBER(s) DNA 001-75-C-0179 <i>new</i>	9. PERFORMING ORG. REPORT NUMBER KA-TR-142
10. PERFORMING ORGANIZATION NAME AND ADDRESS Kaman Avidyne, Division of Kaman Sciences Corp. 83 Second Avenue Burlington, Massachusetts 01803	11. CONTROLLING OFFICE NAME AND ADDRESS Director Defense Nuclear Agency Washington, D.C. 20305	12. PROGRAM ELEMENT, PROJECT, TASK AREA & WORK UNIT NUMBER NWED Subtask N99QAXAE510-21
13. MONITORING AGENCY NAME & ADDRESS (if different from Controlling Office)	14. REPORT DATE Jul 1977	15. NUMBER OF PAGES 78
16. DISTRIBUTION STATEMENT (of this Report) Approved for public release; distribution unlimited.	17. DISTRIBUTION STATEMENT (of the abstract entered in Block 20, if different from Report)	18. SECURITY CLASS. (of this report) UNCLASSIFIED
19. SUPPLEMENTARY NOTES This work sponsored by the Defense Nuclear Agency under RDT&E RMSS Code B342076464 N99QAXAE51021 H2590D.		
20. KEY WORDS (Continue on reverse side if necessary and identify by block number) Blast Overpressure Response Thermal Response Internal Pressurization Nuclear Effects Structural Dynamics		
21. ABSTRACT (Continue on reverse side if necessary and identify by block number) A study of the effects of thermal/blast exposure on representative aircraft panels was carried out jointly by Kaman Avidyne and the Naval Surface Weapons Center. Pre-test planning and analytic predictions were carried out at Kaman Avidyne employing the DNA 2048 methods, and were compared with the experimen- tal results obtained at NSWC. Correlation with experimental results was good for the individual effects of internal pressurization or blast overpressure on panels, but correlation proved to be a difficult task for experiments involving thermal exposure, which have a low confidence level.		

DD FORM 1 JAN 73 1473 EDITION OF 1 NOV 65 IS OBSOLETE

UNCLASSIFIED

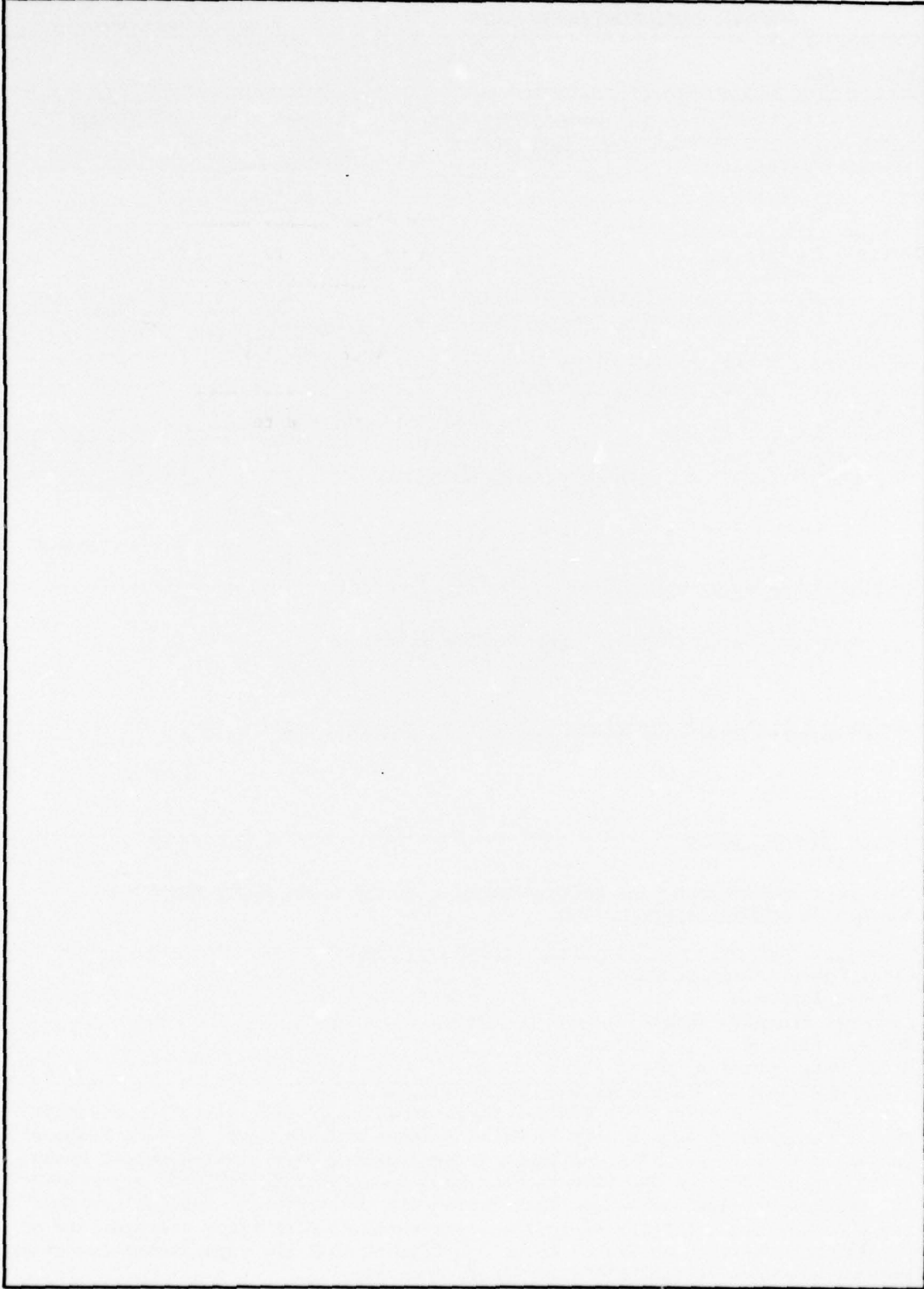
SECURITY CLASSIFICATION OF THIS PAGE (When Data Entered)

194 970

Lee

UNCLASSIFIED

SECURITY CLASSIFICATION OF THIS PAGE(When Data Entered)



UNCLASSIFIED

SECURITY CLASSIFICATION OF THIS PAGE(When Data Entered)

PREFACE

This report was prepared for the Defense Nuclear Agency under Contract No. DNA001-75-C-0179. The analytical work was carried out in the Structures Group at Kaman AviDyne under the supervision of Mr. Emmanuel S. Criscione. Major David W. Garrison was the DNA Contracting Officer's Representative. Mr. Neal Griff was Project Leader for the experiments carried out at the Naval Surface Weapons Center. Their guidance and assistance, as well as contributions from the technical staff at Kaman AviDyne is deeply appreciated.

ACCESSION for		
NTIS	Write Section	<input checked="" type="checkbox"/>
DDC	Buff Section	<input type="checkbox"/>
UNANNOUNCED		<input type="checkbox"/>
JUSTIFICATION		
BY		
DISTRIBUTION/AVAILABILITY CODES		
Dist.	Avail.	and/or SPECIAL
A		

Conversion factors for U.S. customary
to metric (SI) units of measurement.

To Convert From	To	Multiply By
British thermal unit (thermochemical)	Joule(J)	1.054 350 X E+3
degree (angle)	radian (rad)	1.745 329 X E-2
degree Fahrenheit	degree kelvin (K)	$T_K = (T_F + 459.67) / 1.8$
foot	meter (m)	3.048 000 X E-1
inch	meter (m)	2.540 000 X E-2
kilotons	terajoules	4.183
pound-force (lbf avoirdupois)	newton (N)	4.448 222
pound-force/inch ² (psi)	kilo pascal (kPa)	6.894 757

TABLE OF CONTENTS

	<u>Page</u>
I. INTRODUCTION	7
II. PRE-TEST CALCULATIONS.....	9
2.1 Introduction.....	9
2.2 DNA 2048 Methods Employed.....	10
2.2.1 Overpressure Analysis.....	10
2.2.2 Thermal Analysis, With and Without Internal Pressurization	11
2.2.3 Thermal-Overpressure Coupling Analysis	11
2.2.4 Static Internal Pressurization	12
2.2.5 Dynamic Response due to Blast Overpressure...	13
2.2.6 Temperature History due to Thermal Exposure..	13
III. THE EXPERIMENTAL PROGRAM	14
3.1 The NSWC Thermal/Blast Simulation Facilities	14
3.2 The Experimental Set-Up.....	15
IV. PRESENTATION OF RESULTS AND CORRELATION	17
4.1 Introduction	17
4.2 Analytical Results.....	17
4.2.1 Blast Overpressure, Temperature Rise, and Internal Pressurization Effects on Incipient Yield	17
4.2.2 Static Internal Pressure and Dynamic Overpressure on Beam Element	19
4.2.3 Temperature History and Distribution	20
4.3 Experimental Results and Correlation	21
4.3.1 Static Internal Pressurization	22
4.3.2 Blast Overpressure	24
4.3.3 Thermal Exposure Alone or Combined With Blast Overpressure	26
V. CONCLUSIONS AND RECOMMENDATIONS	29
REFERENCES	31

LIST OF TABLES

<u>Table</u>		<u>Page</u>
1	Results Obtained with DNA 2048 Methods, 2024-T3 Aluminum Panels, Sure-Safe Conditions, 10.0x15.0 Inch Rectangular Panels, Clamped Edges	32
2	Results Obtained With DNA 2048 Methods, 2024-T3 Aluminum Panels, Sure-Safe Conditions, 15.0x15.0 Inch Square Panels, Clamped Edges	34
3	Results Obtained with DNA 2048 DEPROB Method, 2024-T3 Aluminum, Elastic/Plastic Response, 10.0 Inch Long Clamped Beam Element From Rectangular Panel	36
4	Experiments on 2024-T3 Aluminum Panels, Clamped Edges, 15.0x15.0x0.50 In. or 10.0x15.0x0.032 In. Exposed Size	37
5	Sample Overpressure Data Reduction	40

LIST OF ILLUSTRATIONS

<u>Figure</u>		<u>Page</u>
1	Effect of Plate Thickness on Temperature Rise or Blast Overpressure Required for Incipient Edge Yielding	41
2	Combined Effects of Temperature Rise and Blast Overpressure Required for Incipient Edge Yielding	43
3	Combined Effects of Temperature Rise and Internal Pressurization Required for Incipient Edge Yielding	45
4	Effect of Plate Thickness on the Combined Effects of Thermal/Pressurization Exposure Required for Incipient Edge Yielding	47
5	Deflections and Strains Obtained from the Beam Element Model Subjected to Static Pressure	48
6	Center Deflection History for Beam Element Models Subjected to Blast Overpressure	50
7	Temperature History and Distribution at Centerline of Square Panels Subjected to Thermal Exposure with a Small Heat Sink at Edge	52
8	Temperature History and Distribution at Centerline of Square Panels Subjected to Thermal Exposure with a Large Heat Sink at Edge	54
9	The NSWC Explosively Driven Conical Shock Tube with Thermal Exposure Provision	56
10	Strain Gage and Thermocouple Locations on Inner Surface for Thermal Exposure Cases	58
11	Strain Distribution on Centerline of Test Panels Subjected to Static Internal Pressurization	59
12	Strain Data in Comparison with Analytical Results for Rectangular Panels Subjected to Static Internal Pressurization	61

LIST OF ILLUSTRATIONS (CONCL'D)

<u>Figure</u>		<u>Page</u>
13	Deflections at Center of Panels Subjected to Static Internal Pressurization	63
14	Strain Distribution on Centerline of Square Panels Subjected to Blast Overpressure	64
15	Strain Distribution on Longer Centerline of Rectangular Panels Subjected to Blast Overpressure	65
16	Strain Distribution on Shorter Centerline of Rectangular Panels Subjected to Blast Overpressure	66
17	Strain Distribution on Inner and Outer Surfaces of Square Panels Subjected to Blast Overpressures.	67
18	Maximum Deflection at Center of Panels Subjected to Blast Overpressure	68
19	Temperature Distribution on Both Center Lines of Square Panels Subject to Thermal Exposure Prior to Arrival of Blast Overpressure	69
20	Strain Distribution on both Centerlines of Square Panels Subjected to Combined Thermal/Blast Overpressure Exposure.....	70

SECTION I

INTRODUCTION

In previous work, Kaman AviDyne has consolidated into a user-oriented document various analytical methods, either simple or complex in their approach, for predicting the response of aircraft structures to the thermal radiation and subsequent blast wave associated with a nuclear detonation. Sure-safe and sure-kill criteria are determined. The original document was recently revised to incorporate the latest techniques developed since its original publication, and was issued as DNA 2048 (Reference 1). Among the revisions incorporated in the report were the following: 1) A method for predicting the response of an internally-pressurized aircraft skin panel subjected to the thermal radiation of a nuclear detonation, and 2) A method for predicting the response of an internally-pressurized aircraft skin panel subjected to the thermal radiation and subsequent blast wave exposure due to a nuclear detonation.

Kaman AviDyne has also developed the NOVA (Nuclear Overpressure Vulnerability Analysis) overpressure code (Reference 2). This code is also cited in DNA 2048 as a complex solution method. Two routines in the NOVA code, DEPROB and DEPROP (Dynamic Elastic/Plastic Response of Beams, and of Panels, respectively) have the capability of analyzing overpressure loading or internal pressure, or their combined effects. A modification of these routines to include thermal exposure effects, via provisions for material degradation and thermal strain, was carried out to accommodate arbitrary spatial temperature distribution. The modified codes thus were capable of treating combined effects of thermal/ blast exposure of pressurized panels with the response extending into the plastic range.

Experimental verification of the results obtained by employing the analytical prediction methods cited above was desired. The facilities and capabilities of carrying out experiments on pressurized panels subjected to either thermal exposure or blast overpressure, or their combined effects, exist at the Naval Surface Weapons Center (NSWC),

at White Oak, Silver Spring, Maryland. Under DNA sponsorship, a joint program was undertaken utilizing the Kaman Avidyne analytical capability and the NSWC experimental facilities and expertise to devise an experimental program which would assist NSWC in the further development of their thermal/blast exposure simulation techniques and provide the necessary experimental data for use in the verification of the analytical predictive methods at Kaman Avidyne. Pre-test calculations, employing the DNA 2048 analytical methods, were carried out at Kaman Avidyne to plan the suggested sequence of tests and exposure levels. The experiments, with associated data recording and reduction, were then carried out at NSWC, and the results were then analyzed and correlated at Kaman Avidyne.

The pre-test calculations on selected representative aircraft panels and the analytical methods employed are described in the next section, Section II. A description of the experimental program and the facilities is presented in Section III. Section IV presents the data reduction and the confidence associated with the experimental results as well as the predictive capabilities of the analytical methods and the correlation of results. Finally, Section 5 presents the conclusions and recommendations for further work.

SECTION II

PRE-TEST CALCULATIONS

2.1 Introduction

The joint effort of studying thermal/blast effects on typical aircraft structures was shared by Kaman AviDyne and the Naval Surface Weapons Center (NSWC). Kaman AviDyne had the responsibility of pre-test planning and determination of typical structures to be tested under specified exposure levels. NSWC was to carry out the experimental testing program and associated data recording and reduction for subsequent correlation with analytical predictions at Kaman AviDyne

Kaman AviDyne examined the structural characteristics of typical aircraft skin panels, and with due consideration to the size and exposure level limitations of the experimental facility, determined the panel material, size, and support configurations of interest. The test panels were selected to be made of 2024-T3 aluminum, clamped rigidly at the perimeter such that a square flat panel measuring 15.0 in. by 15.0 in. or a rectangular flat panel measuring 10.0 in. by 15.0 in. was available for exposure to the thermal radiation and/or blast overpressure. Provision was also made for subjecting the panels to internal pressurization of a magnitude typical for aircraft.

The initial phase of the analytical study, employing the methods of DNA 2048, was restricted to sure-safe conditions, defined as a level of response corresponding to incipient damage. For the case of skin panels, the sure-safe criterion is the onset of yield. When the panels are rigidly clamped at the perimeter and subjected to the types of loading under consideration, incipient yield will occur on the panel surface at the clamped edge.

Although the combined effects of internal pressure/thermal radiation/blast overpressure were of interest in this study, the individual exposure effects were also studied to provide basic cases for the validation checks of the results, both analytical and experimental.

For the second phase of the analytical study, employing the modified DEPROB and DEPROP codes with elastic/plastic response capability, higher exposure levels were employed to obtain responses well beyond the elastic limits of the material, with the aim of obtaining visible permanent damage of the panel but avoiding rupture.

2.2 DNA 2048 Methods Employed

The relatively simpler methods employed for this study in DNA 2048H-1 are restricted to flat panels under sure-safe conditions. The iterative methods employed adjust the exposure levels until the response converges to the condition where a fiber on the surface of the panel, at the clamped edge, has just reached the specified yield stress level. This incipient yield criterion places a rather stringent sure-safe condition, admittedly difficult to simulate experimentally. Since the DNA 2048 methods are intended to provide envelopes for the sure-safe condition of interest, the iteration technique varies the range between aircraft and blast center to obtain the desired response, and determines the exposure levels for that range. Hence, weapon yield is a primary input, with temperature rise and blast overpressure calculated based on weapon yield and ambient conditions.

Brief descriptions of the DNA 2048H-1 methods employed in the different phases of the study follow. The results are presented in Figures 1 through 8 and discussed in Section IV.

2.2.1 Overpressure Analysis

For the analysis of panels subjected to the individual effect of blast overpressure, the method described in DNA 2048, Appendix C1.2, Method 2, Part A, "Overpressure Effects on Single Layer Skin Panels" was employed. The major assumptions of panels being thin, flat, rectangular, rigidly-clamped, free from pre-blast stresses, and surrounded by a homogeneous pre-blast environment, were satisfied. Ground altitude and aircraft altitude were specified as zero for an approximation of the ambient conditions at the NSWC test site. Both the square (15 x 15 in.) and the rectangular (10 x 15 in.) panel sizes selected were employed, and the thickness of the test panels

was varied from 0.032 to 0.072 in. For the yield criterion, two values of yield stress were employed to bracket possible material properties: 42,000 and 48,000 psi. The computerized version of the solution method, program OVPR2, was used for the generation of data.

2.2.2 Thermal Analysis, With and Without Internal Pressurization

For the analysis of panels subjected to the individual effect of a temperature rise due to thermal radiation from a nuclear blast, as well as the combined effects of internal pressurization of a panel subjected to a temperature rise, the method described in DNA 2048, Appendix D1.2, Method 2, "Thermal Radiation Effects on Aircraft" was employed. The major assumptions that were satisfied include the following: flat, rectangular, rigidly-clamped panels free from pre-blast stresses, uniform heating of panel and no heating of supports. The surface finish, which affects absorbtivity, was specified to be unpolished aluminum. Both square and rectangular panel sizes were employed, with a thickness range from 0.032 in. to 0.072 in. The values of yield stress employed were 42,000 and 48,000 psi, with a limited investigation of the effect of a 50,000 psi yield stress to bracket the possible range of values for the material. Internal pressurization was set at zero for the pure thermal effect study, and ranged from 1.0 psi to 6.0 psi for the combined effects of internal pressurization and temperature rise. The computerized version of the solution method, program THERM2, was used for the generation of data.

2.2.3 Thermal-Overpressure Coupling Analysis

For the analysis of panels subjected to the combined effects of thermal radiation and blast overpressure exposure from a nuclear blast, the method described in DNA 2048, Appendix I1.2, Method 2, Part A, "Thermal-Overpressure Coupling Effects on Single-Layer Panels" was

employed. The major assumptions that were satisfied are identical to those described in Subsection 2.2.2. Surface finish for the panels was unpolished aluminum. Again, the study employed both the square and the rectangular panel sizes with thickness ranging from 0.032 in. to 0.072 in. Again, values of 42,000 psi. and 48,000 psi. were employed for yield stress. In all cases, the internal pressure was set at zero, since the thermal-overpressure coupling alone was of interest. Weapon yields ranging from 0.1 to 1,000 kilotons were used in the study. Since the study iterates to determine the range at which a given weapon yield causes the incipient yield condition, the temperature rise and overpressure at the appropriate range for each given weapon yield are calculated as dependent quantities. The smaller weapon yield places the burst center closer to the structure being analyzed; as weapon yield is increased, the range at which incipient yield of the panel occurs increases, resulting in increased temperature rise for the panel but smaller blast overpressure on the panel. The computerized version of the solution method, program OPTC, was used for the generation of data.

2.2.4 Static Internal Pressurization

A limited study was made to determine the individual effect of static internal pressurization, to provide a basis for comparison with the study of cases where internally-pressurized panels were subjected to thermal radiation. A beam element model, representing a slice cut from the rectangular panel along its shorter dimension centerline, was used for this study. Because of the length-to-width ratio of the rectangular panel ($15/10 = 1.5$), this 10-in. long beam element model will approximate the response of the panel along the shorter dimension centerline, where the higher magnitudes of strain will exist. A simplified version of the DEPROB routine was employed to generate the data. The solution is obtained from the dynamic code by iteration until a static equilibrium is obtained. Static internal pressures of 2, 3, and 4 psi were imposed.

2.2.5 Dynamic Response due to Blast Overpressure

A limited study was also made to determine the dynamic response resulting from the individual application of blast overpressure. The response extended beyond the yield limits and into the plastic deformation range. The beam element model employed represented a slice cut from the rectangular panel along its shorter dimension centerline, as the higher magnitudes of strain occur along that centerline. The simplified version of the DEPROB routine was employed to generate the data. Blast peak overpressures ranging from 2.0 psi. to 25.3 psi. were used.

2.2.6 Temperature History due to Thermal Exposure

A limited investigation was carried out to determine the temperature history and distribution of test panels due to thermal exposure from a blast. A relatively small and a relatively large heat sink, compared to panel size, was used to model the effect of conduction paths through the frame used for clamping the panels in the experimental set-up. The model employed represented a strip cut from the square panel along a centerline, connected to the heat sink selected (shielded from radiant exposure). The TRAP program (Reference 3) also presented as a complex solution in DNA 2048, Appendix D1.3, Method 3, was employed to generate the data. The thermal exposure consisted of a heat input of 0.1 Btu/sec for each square inch of exposed area, for a duration of 2.0 sec.

SECTION III

THE EXPERIMENTAL PROGRAM

3.1 The NSWC Thermal/Blast Simulation Facilities

The development of the NSWC test facilities for the simulation of nuclear thermal/blast exposure are described in Reference 4. The NSWC explosively driven Conical Shock Tube (CST) is shown schematically in Figure 9. The CST is used to simulate the blast effects of large explosions by generating a sector of a spherical blast wave which travels axially along the divergent steel tube, thus producing a blast wave with an observed amplification of 30,000 compared to the free-air blast from the same amount of Primacord explosive. The test station is at a distance of 225 feet from the center of the explosion. Blast overpressures are measured via pressure transducers on the shock tube sidewall for incident pressure, or the end plate at the test section for reflected pressure.

The thermal exposure simulation is achieved by the rapid heating of test samples due to the combustion products of specially formulated propellant sheets. The propellant sheets may be formed to various thickness specifications. They are placed on sheets of insulating transite for support, and ignited by an imbedded gridwork of nickrome wire heated to incandescence.

The thermal exposure source is mounted just ahead of the test section in the proximity of the test sample. Upon ignition, the hot combustion product gases impinge on the test sample for rapid convective heating. With appropriate timing, the jig holding the thermal source is released to drop the propellant backing sheet out of the way and replace the cut-away section of the shock tube with a sealing ring, prior to the arrival of the blast wave. The detail of the test section is shown in Figure 9.b.

In addition to the pressure transducers, provisions are made to record the output from strain gages and thermocouples mounted on the test specimens, or the output of a non-contacting proximity gage for the measurement of deflections.

3.2 The Experimental Set-Up

Based on the pre-test calculations made at Kaman AviDyne, as discussed in the preceding Section II, the test panels were selected and appropriate support configurations, gage placements and test sequences were recommended to NSWC. The test panels were made of 2024-T3 aluminum and were clamped at the perimeter such that either a square flat panel measuring 15.0 x 15.0 inch or a rectangular flat panel measuring 10.0 x 15.0 in was available for exposure to the thermal radiation and blast overpressure. The thickness of the square panels was 0.050 in., and the thickness of the rectangular panels was 0.032 in. The test section was also sealed aft of the mounted test panels to enable "internal pressurization" of the test panels. The selected test series was designed to study the effects of thermal exposure, blast overpressure, or internal pressurization individually or their combined effects.

The test section was modified to accept either of two thick steel plate bulkheads, designed to be attached to the existing flange of the test section. One bulkhead had a square cut-out to accommodate the square test panels, and the other had a rectangular cut-out to accommodate the rectangular test panels. The test panels were cut oversize such that a one-inch wide section around the perimeter would fit into a step milled out of the bulkhead. A separate inch-wide steel frame was fitted over the panel, and bolts going through the frame/panel/bulkhead clamped the assembly together, in an attempt to provide a rigid non-rotating boundary condition for the panels.

The above-described clamping arrangement of course had direct metal-to-metal contact between the mounted test panel and surrounding frame. At the expense of some loss of rotational rigidity of the clamped boundary condition, selected tests were also carried out on panels which had insulating strips of transite sandwiched between the panel and the bulkhead or frame contact surfaces. This was an attempt to thermally isolate the test panels from the surrounding

frame to reduce the "heat sink" effect of the frame surrounding a heated panel. In addition, panels were non-destructively tested mounted in one position, then removed and re-mounted inverted (up-side down) to check on the possibility of warped frame, misalignment, or bolt torque effects on mounted test panels.

Recommended instrumentation included the following: a pressure transducer on the bulkhead near the test panel to measure reflected blast overpressure in addition to the incident pressure measurement provided by the pressure transducer on the shock tube wall; strain gages placed on both surfaces of test panels at specified stations close to the clamped edges for test panels not subjected to thermal exposure; strain gages and thermocouples on the shielded surface of test panels subjected to thermal exposure; a pressure regulating system and pressure gage for the internal pressurization of the test panels; and a non-contacting variable impedance transducer (Kaman Sciences KD-2300-10CU) for measurement of displacement history at the center of the test panels.

SECTION IV

PRESENTATION OF RESULTS AND CORRELATION

4.1 Introduction

The results of the pre-test calculations, the data obtained from experiments based on the recommended test plan, results of post-test calculations, data reduction and correlation of analytical and experimental results are presented in this section.

The selection of the test panels and analytical methods of solution are described in the preceding Section II, and the experimental methods are described in the preceding Section III.

4.2 Analytical Results

4.2.1 Blast Overpressure, Temperature Rise, and Internal Pressurization Effects on Incipient Yield

The DNA 2048 methods described in the preceding Section II were employed to determine the levels of blast overpressure, temperature rise, internal pressurization, and their combined effects, which would subject the selected panels to incipient yielding at the clamped edges.

Tables 1 and 2 present the full set of cases studied with the 10.0 x 15.0 inch rectangular panels and the 15.0 x 15.0 inch square panels, respectively. The cases are identified with code letters and numbers as follows: prefix R for Rectangular panels, or prefix S for Square panels, O for Overpressure, T for Temperature rise, P for internal Pressure, followed by an abbreviated numerical code to indicate panel thickness, yield stress, and weapon yield or internal pressurization, which are tabulated in the following four columns of the tables. Blast overpressure (incident and reflected), and the temperature rise needed for the onset of edge yielding are also tabulated. Unpolished aluminum surface condition is used except where specified polished or non-absorbing surface finish is indicated. Surface finish affects thermal absorbtivity and temperature rise.

The results shown in Tables 1 and 2 are presented graphically in Figures 1 through 4. Figure 1.a shows the effect of plate thickness and various yield stresses on the temperature rise for incipient edge yielding, and Figure 1.b shows the effect of the same parameters on the blast overpressure for incipient yielding. It is noted that the thicker panels yield at higher blast overpressures, but thicker panels require a lower temperature rise for the onset of yielding at the outer fibres of the edge. This effect is explained by the fact that the thicker panels have fibers further away from the neutral axis that will have larger stresses for the same buckled shape of the panel due to a constant temperature rise. Higher yield stresses naturally require larger blast overpressure or temperature rise for incipient yielding.

Figures 2.a and 2.b show, for the square panels and the rectangular panels respectively, the combined effects of a temperature rise and blast overpressure to cause incipient yielding for different panel thicknesses and yield stresses employed. Similarly, Figures 3.a and 3.b show the combined effects of a temperature rise and internal pressurization to cause incipient yielding. Since temperature rise and blast overpressure are the results of the same burst, relative magnitudes for the study can be obtained by varying the weapon yield (and allowing the program to iterate on an appropriate range for the sure-safe criterion). Larger weapon yields at longer ranges result in higher temperature rises and lower blast overpressures, as shown in Figure 2. It should be noted that when the overpressure is zero in Figure 2, or when the internal pressure is zero in Figure 3, the ordinate shows the individual effect of temperature rise for incipient yielding. Similarly, when the temperature rise is zero in Figure 2, the abscissa shows the individual effect of blast overpressure for incipient yielding. Incipient yielding due to internal pressure alone was not investigated.

Figure 4 shows the same information depicted in Figure 3 but using plate thickness as the abscissa. The figure clearly shows the trend that the presence of internal pressurization imposes the need for

higher temperatures for incipient yielding of thicker panels, whereas the absence of internal pressurization has the reverse effect explained earlier in connection with Figure 1.a. Of course, larger values of internal pressure require lower temperature rise for incipient yielding for given panel thicknesses, and a material with larger yield stress requires a higher temperature for incipient yielding.

4.2.2 Static Internal Pressure and Dynamic Overpressure On Beam Element

The DEPROB method of DNA 2048 described in Section II was employed for a limited study of the effects of static internal pressure and the dynamic response to blast overpressure acting on a representative beam element model. The beam element model represented a strip of the rectangular plate, on the shorter dimension of the rectangle centerline. The 10.0 inch long beam was clamped at both ends. It was subjected to uniformly distributed loads equivalent to static internal pressures on the plate, or subjected to dynamic loading of stated values of blast peak overpressures, or subject to dynamic overpressure loading which was iterated to determine the peak overpressure required for incipient yielding of the outboard fibres at the clamped edges.

Table 3 shows the full set of cases studied with the 10.0 inch beam element model. The cases are identified with code letters and numbers as follows: prefix BR for Beam element from Rectangular panel, S for Static internal pressure, D for Dynamic overpressure, and I for Iteration to determine onset of yield, followed by an abbreviated numerical code to indicate panel thickness, yield stress, and static or dynamic overpressure level, which are tabulated in following columns. The iterated dynamic peak overpressure to cause the onset of edge yielding is tabulated under the heading ΔP_y . Also shown are the peak deflection at the center and the time at which it occurs, as well as the time for the onset of edge yielding, where applicable.

It should be noted that the BRD cases are not iterated with other levels of overpressure, and hence represent the dynamic response for the given peak overpressure $\Delta P_{\theta=0^\circ}$, whereas the BRDI cases are iterated with various peak overpressures until a no-yielding/onset-of-yielding situation is bracketed with the magnitudes of the peak overpressures shown under the heading ΔP_y .

Selected results shown in Table 3 are presented graphically in Figures 5 and 6. Figure 5.a shows the deflection for the half-span of the beam model for different thicknesses and applied equivalent static internal pressure loading, and Figure 5.b shows the strains at the surface fibers on the loaded side for the same configurations. Note that the thinner model exhibits mostly membrane type behavior, whereas the thicker model exhibits the bending strain contribution at the center, especially for the 3 psi case where net compressive strains exist for the outer fibre on the loaded side.

Figure 6 shows the time histories of the deflections at the center of the 0.032 inch thick beams subjected to various peak blast overpressures. The blast overpressure pulses are triangular in shape, with decay times much greater than the response times shown, and hence approximate the effect of a step pulse input. The indicated tick marks on the curves show the times where edge yielding was first observed, as recorded in Table 3. None of the computer runs were carried out far enough in time to determine the permanent set deflection of the beam element models.

4.2.3 Temperature History and Distribution

The TRAP method of DNA 2048 described in Section II was employed for a limited investigation of the temperature history and distribution in a representative beam element model to determine the effect of heat sinks at the clamped edges. The beam element model represented a strip of the square plate on its centerline. The 15.0 inch long beam element was connected to either of two lumps of material at each end, shielded from thermal exposure and intended to act as heat sinks.

The effort was to model possible extremes of conduction paths at the frame structure into which the test panels were clamped for the experiments. The relatively small heat sink was essentially a one-inch extension of the 0.05 inch thick beam model, equal to the segment of the test panel held inside the clamping frame and shielded from thermal exposure. It represented an ideal insulation between test panel and clamping frame. The relatively larger heat sink increased ten-fold the thickness of the beam in the shielded region to 0.5 inch, to represent a good conduction path between the panel and its clamping frame.

Figures 7 and 8 depict the results of the thermal exposure investigation for the small and large heat sink cases, respectively. Figures 7.a and 8.a show the temperature rise/absolute temperature histories at given stations for both cases, while Figures 7.b and 8.b show the temperature distribution at given instants of time for both cases. A comparison of the results for both heat sink cases indicates that away from the edge there are negligible differences in temperature history and distribution. Neglecting station 1, centrally located within the heat sink in the shielded segment of the model, only station 2 (one-half inch away from the clamped edge) shows a slightly accelerated drop in temperature for the larger heat sink.

It should also be observed that, during the application and up to the termination of heat, the temperature distribution for both cases is nearly uniform. There is quicker degradation of the edge temperature during the cool-down period, as the heat sink temperature rises.

4.3 Experimental Results and Correlation

Based on the results of the pre-test calculations and up-dated calculations as the experiments progressed, a test program was recommended by Kaman AviDyne and carried out at NSWC. The results of the experiments were recorded, the data was reduced and transmitted by NSWC to Kaman AviDyne for correlation with the analytical results.

Table 4 presents the full set of experiments carried out at NSWC. The first three columns in the table show the identifying test numbers under the NSWC or Kaman Avidyne notation, and whether the tested panels were the square 15.0x15.0x0.050 inch thick, or the rectangular 10.0x15.0x0.032 inch thick panels. The following three columns give the static internal pressurization, the temperature rise, or the blast overpressure experienced by the panels, with an entry in more than one column indicating a combined effects test. The next column shows the panel mounting configuration; no entry means that the panel was rigidly clamped in the frame under metal-to-metal contact, "insulated" means that a thermal insulation strip of transite was sandwiched between the panel and frame, and "inverted" means that the panels tested previously were removed and re-mounted upside-down for a check of repeatability of results. The last column indicates whether strain gages or thermo-couples were installed on the test panels, whether they were on the inner or outer (exposed) surfaces of the panels, and the centerline axes that were instrumented. When a test panel was not intended to be subjected to thermal exposure, it was instrumented on both surfaces with strain gages; for thermal exposure cases, only the inner surface was instrumented with strain gages and thermocouples. The gages were located on or near the centerlines of the test panels, as shown in Figure 10. The figure also shows the location of the non-contacting displacement gage target area at the center of the test panel for measurement of center deflections.

Selected results from the experiments shown in Table 4 are presented and discussed below.

4.3.1 Static Internal Pressurization

Figures 11.a and 11.b present the strain along the centerline for the rectangular and the square test panels, respectively, subjected to 2 or 4 psi static internal pressure. The same panels are mounted with insulation strips, or without insulation strips, or inverted

from the latter configuration. The plotted results are obtained from the strain gages on the inner (pressurized) or outer surfaces. Also marked on the plots is the yield strain, ϵ_y , of the material.

Variations in the strain results due to mounting configuration are noticed, as well as variations when the same test is carried out on a different panel (the repeated symbols). It should be noted that strains extrapolated to the clamped edge station on the pressurized surface show tensile strains at or slightly in excess of yield strain values for the shorter dimension centerline of the rectangular panel in Figure 11.a. Reference to the analytical calculation results shown in Figure 3.b confirms that the appropriate extrapolated curve for the 0.032 inch thickness panel intersects the abscissa (zero temperature rise, or pure internal pressure effect) before 4 psi for the assumed $\sigma_y = 42,000$ case indicating the onset of yield. Conversely, in Figure 11.b no curve reaches yield strain for the square panel subjected to 4 psi internal pressure, as borne out by the results shown in Figure 3.a.

In Figure 12, the strain information for the rectangular panels subjected to 2 psi internal pressure is also shown superposed on the analytical results shown earlier in Figure 5.b. The symbols plotted in Figure 12.a are for the 0.032 inch thick panel under 2 psi static internal pressure (solid curve) and the symbols plotted in Figure 12.b are for the 0.032 inch thick panel under 4 psi static internal pressure (medium dashed curve). The correlation becomes poorer near the clamped edge, and the scatter in the experimental results tends to exceed the variation in the analytical results in going from 2, to 3, to 4 psi internal pressure. Since the onset of yield occurs at a clamped edge, the scatter in the experimental results under easily-controlled static conditions raises the question whether strain gages placed near the edge are reliable as indicators of inception of yield.

A similar scatter in the experimental results is observed for the deflection at the center of the panels, as shown in Figure 13.

Results for both rectangular and square panels are shown for the three noted mounting configurations, as well as the beam-element model analytical results from the DEPROB method of DNA 2048, as obtained from results depicted earlier in Figure 5.a. The panels mounted with insulating strips (round symbols) do give the largest center deflection, as expected, because the boundary condition becomes a softer clamp that may allow rotation. It is noteworthy that the metal-to-metal clamped cases (square and triangle symbols), although exhibiting lack of repeatability, generally do follow the same slope in going from 2 to 4 psi internal pressure. It is thus conceivable that mounted panels may have a warp, or be non-planar, and may pop into a certain position upon application of internal pressure. Once that discontinuity is overcome, increasing pressure apparently increases center deflection at the same rate.

4.3.2 Blast Overpressure

The determination of the blast overpressure was based on the time history of the recorded traces from pressure transducers in the shock tube. A pressure transducer mounted on the tunnel wall near the test section registered side-on or incident pressure, and a pressure transducer mounted on the bulkhead supporting the test panels registered face-on or reflected pressure. Table 5 presents sample data reduction steps leading to the determination of mean and peak overpressures due to a blast, based on measurements from recorded traces. Test number and pressure gage locations are identified, calibration values for gages are shown, and the measured deflections (in) on the traces are tabulated showing the calibration step and the observed mean and peak overpressures. The preceding information is used to calculate the quantities PKA, as shown, which in turn are translated from calibration charts to values of overpressure in psi units.

Similar data reduction steps are followed to obtain strains on the test panel surfaces, based on recorded output traces from strain gages mounted on the test panels subjected to the blast overpressures.

Figure 14 presents the strain along a centerline of the square test panels subjected to various blast overpressures, and Figures 15 and 16 present the strain along the longer and the shorter centerlines, respectively, of the rectangular test panels subjected to various blast overpressures, as determined in Table 5. The strain gages for this test series were placed only on the inner surface on both centerlines. The bending due to the blast overpressure results in tensile strains, due to membrane action, at stations away from the clamped edges, but the compressive strains on the inner surface, due to bending at the clamped edges, overcome the membrane strains and result in net compressive strains. In Figures 14 through 16 the tensile strains are shown as positive values and the compressive strains as negative values, the set of lower right hand curves. The upper right hand curves (dashed) represent an estimate of the net strains on the outer (exposed) surface of the test panels by reflecting the strain curves about an estimated pure membrane action strain. Later, series of tests were carried out with instrumentation placed properly on both surfaces. Figure 17 presents selected results from the later series, indicating the validity of the earlier estimated curves.

It is obvious that incipient yielding will occur on the outer surface of the panels exposed to the blast overpressure, at the clamped edge boundary where tensile strains are additive for the membrane and bending actions. Reference to the earlier-described analytic results of Figures 2.a and 2.b indicate that, for pure blast overpressure (points on the abscissa) the 0.050 inch thick square panels are expected to start yielding at the clamped edge at overpressures of 1.52 or 1.84 psi for assumed yield stresses of 42,000 or 48,000 psi, respectively; similarly, the 0.032 inch thick rectangular panels are expected to yield at overpressures of 0.99 or 1.21 psi. The experimental results shown in Figure 14 indicate estimated onset of yield near an overpressure of 2.29 psi. for the square panel. The lowest blast overpressure for the rectangular panel, shown in Figure 16, is 2.92 psi and has resulted in yielding even at points away from the clamped

edge. The results shown in Figure 17 for the square panel indicate onset of yield at an overpressure between the shown 1.7 psi and 3.1 psi results. Since the strain gage closest to the clamped edge is 1/8 inch away from the actual boundary, the extrapolation of the curves may be subject to question, and the idealized clamped boundary may also be a far-fetched assumption. Nevertheless, properly placed strain gages near the edge seem to provide adequate information to indicate the onset of yield at overpressures generally in the range of levels expected from the analytic predictions.

Maximum center deflections recorded for panels subjected to blast overpressures are shown in Figure 18. Results for the rectangular and square panels are shown for three different data reduction sources, as identified in the figure. Also shown are the analytic results obtained with the DEPROB method of DNA 2048 for the rectangular panels. The experimental results for the rectangular panels show smaller deflections than expected from the analytic predictions, especially for higher blast overpressures. There is also relatively large scatter in the experimental results, possibly due to the effects of clamping or initial warp of panels, as discussed earlier for the presentation of results of the static internal pressure tests.

4.3.3 Thermal Exposure Alone or Combined With Blast Overpressure

Determination of temperatures on the test panel was based on the output from thermocouples attached to the inner (shielded from thermal exposure) surface of the panels, on or near the centerlines and at distances 1/4 inch from the edges, also near the panel center (to avoid interference at the target area of the center deflection gage).

Figures 19.a and 19.b present the recorded temperature rises just prior to the arrival of the blast overpressure, for the square panels along centerlines going from top to bottom, and left to right, in the mounted position. All of the results exhibit temperature distributions where the panel centers are at temperatures two to three times higher

than the temperatures near the edge, whereas a uniform temperature distribution is assumed in the analytic predictions for onset of yield and is desired for the experiments. Noticeable variations also occur in the same panel for the temperature recorded at four points on the centerlines near the edges at top, bottom, left, and right of mounted panels, where symmetry dictates identical results in theory. Some of the temperature variation is attributable to the convective heating nature of the thermal source, noting that the hot gases may be hindered from adequately reaching the plate edges because of the protruding clamping frame. Also, even though insulating transite strips were used in sandwiching the plates under the clamping frame, some conduction is possible to the bulkier and cooler supporting structure which acts as a heat sink.

Reference to the analytical results shown in Figures 7 and 8 indicates that the predicted temperature variation from edge to center is much smaller than the variation observed in the experimental results, for the assumed small or large heat sink cases, especially when a cool-down period is minimized with the quick arrival of the blast overpressure.

A serious question is thus raised on the reliability of experimental results involving thermal exposure alone, or in combination with internal pressurization or blast overpressure. Especially since onset of yield occurs at the edge, where the largest uncertainty of temperature exists, any attempt at correlation with predicted results will have a low confidence level.

Further evidence of the uncertainty in results for thermal exposure tests is seen in Figures 20.a, 20.b, and 20.c, which show the strains along both centerlines of the square panels subjected to thermal exposure first and then followed by blast overpressure. Where enough data points are available, an attempt has been made to show the estimated strain distribution with long-dashed curves for the thermal exposure alone or the short-dashed curves for the thermal/blast

combined effects. All gages are on the inner surface of the panel, and tensile strains are plotted as positive values. In Figure 20.a, Test 62 results show that the panel bulges towards the thermal source when heated, with tensile strains at the edges and compressive strain at the center; the 1.3 psi blast overpressure causes all strains to be compressive with the panel apparently maintaining its bulged shape. Tests 63 and 64 also show that the panel bulges out toward the thermal source upon heating, but subsequent exposure to the 3.2 or 4.2 psi blast overpressure causes it to pop through to the other side, with the center developing tensile strains. Noting from results presented in Figure 19.a that tests 62-64 have a temperature rise of about 150°F near the panel center, and referring to Figure 2.a, onset of yield is analytically predicted at an approximate blast overpressure of 1.5 psi. The inconclusive results of Figure 20.a seem to be in agreement with the prediction, with the 1.3 psi overpressure case not exceeding the yield strain of 0.45%, but the 3.2 and 4.2 psi overpressure cases exceeding yield strain at the edges. Noting from results presented in Figure 19.b that tests 65-70 have a temperature rise of about 300°F near the panel center, and referring again to Figure 2.a, onset of yield is analytically predicted at an approximate blast overpressure of 1.0 psi. Figure 20.b has an inadequate number of reliable data points to attempt a curve fit. In Figure 20.c, Test 68 results show that the panel bulges towards the thermal source when heated, with tensile strains at the edges and compressive strain at the center, which exceeds the yield strain for the gage near the center in the top to bottom distribution plot. Data points plotted as "center" values do not agree in the vertical and horizontal distribution plots because they are obtained from separate gages which are oriented to measure the strains in the appropriate direction. For the square panels under consideration the strains at the center along both centerline directions should be identical, in theory, for a uniformly heated clamped panel. The application of the 1.35 psi blast overpressure seems to alter the strains slightly. Test 70 results show all strains on the inner surface, due to thermal exposure alone, as compressive strains, with little change upon application of the 1.03 psi blast overpressure.

SECTION V

CONCLUSIONS AND RECOMMENDATIONS

The investigation of thermal/blast effects on selected panels, a joint effort by Kaman AviDyne and the Naval Surface Weapons Center, generated extensive information obtained by analytical methods and data reduced from experimental results. Although the analytical predictions were used to establish a recommended experimental program, and the test results were intended to validate the analytical methods of DNA 2048 developed at Kaman AviDyne, serious problems were encountered in attempts to correlate analytic and experimental results for the thermal/blast combined effects cases.

The preliminary work that was carried out in preparation for the more complex cases investigated the individual effects of internal pressurization, blast overpressure, and thermal exposure. The experimental results compared well with the analytic predictions for the square or rectangular clamped panels subjected to internal pressurization alone or to blast overpressure alone, in efforts to determine the onset of yield in a surface fiber at an edge of the panel. Experiments involving thermal exposure, however were beset with the difficulties of poor temperature distribution in the panels, with rapid drop-off at the clamped edges, as a result of non-uniform impingement of the combustion product gases of the solid propellant thermal source, or the heat-sink effect of the clamping frame around the test panels. Non-repeatability of results and lack of expected symmetry also reduced the level of confidence in the experiments involving thermal exposure. Thus the use of the experimental results to validate the analytical solution methods became questionable.

Future work should be directed to the resolution of the difficulties encountered with the thermal source, so that the level of exposure can be controlled more closely, and the desirable uniformity of heating achieved. Data recording and reduction techniques may also need optimization, to improve the reliability of the results obtained in the admittedly difficult task of measuring temperatures and strains

close to an edge bolted in a supporting frame which may not adequately represent the idealized clamped boundary condition assumed for the analysis. Further, the determination of incipient yielding, where one fiber on the surface of the panel at its clamped boundary just reaches the material yield point, is a stringent test difficult to achieve experimentally.

REFERENCES

1. Hobbs, N.P., et al, Handbook for Analysis of Nuclear Weapon Effects on Aircraft, Volumes 1 and 2, DNA 2048H-1, and DNA 2048H-2, Kaman Avidyne, March 1976.
2. Hobbs, N.P., et al, NOVA - A Digital Computer Program for Calculating the Response of Aircraft to the Overpressure from a Nuclear Explosion, Vol. I, Theory and Program Description, AFWL-TR-72-115, Vol. I, Kaman Avidyne, July 1973.
3. Hobbs, N.P., Wetmore, K.R., and Walsh, J.P., TRAP - A Digital Computer Program for Calculating the Response of Aircraft to the Thermal Radiation from a Nuclear Explosion, Vol. I, Theory and Program Description, AFWL -TR-71-61, Vol. I, Kaman Avidyne, October 1972.
4. Katz, B.S., and Connor, J.G. Jr., Development of the NDL Thermal Blast Simulator, NOLTR 72-183, Naval Ordnance Laboratory, July 1972.

TABLE 1

RESULTS OBTAINED WITH DNA 2048 METHODS
 2024-T3 ALUMINUM PANELS, SURE-SAFE CONDITIONS
 10.0X15.0 INCH RECTANGULAR PANELS, CLAMPED EDGES

CASE I.D.	H IN	σ_y PSI	W KT	P _i PSI	$\Delta P_{\theta=90^\circ}$ PSI	$\Delta P_{\theta=0^\circ}$ PSI	ΔT °F	SURFACE
RO 32,42,1	0.032	42,000	1	0	0.99	1.85	0.0	
RO 32,42,1000	0.032	42,000	1,000	0	0.99	1.85	0.0	
RO 32,48,1	0.032	48,000	1	0	1.20	2.25	0.0	
RO 32,50,1	0.032	50,000	1	0	1.28	2.39	0.0	
RO 50,42,1	0.050	42,000	1	0	1.56	3.01	0.0	
RO 50,42,1000	0.050	42,000	1,000	0	1.56	3.01	0.0	
RO 50,48,1	0.050	48,000	1	0	1.91	3.70	0.0	
RO 50,50,1	0.050	50,000	1	0	2.03	3.93	0.0	
RO 63,42,1	0.063	42,000	1	0	1.92	3.75	0.0	
RO 63,48,1	0.063	48,000	1	0	2.34	4.58	0.0	
RT 32,42,1	0.032	42,000	1	0	0.00	0.00	601.0	
RT 32,42,1000	0.032	42,000	1,000	0	0.00	0.00	601.0	
RT 32,48,1	0.032	48,000	1	0	0.00	0.00	623.8	
RT 32,50,1	0.032	50,000	1	0	0.00	0.00	630.5	
RT 50,42,1	0.050	42,000	1	0	0.00	0.00	533.5	
RT 50,48,1	0.050	48,000	1	0	0.00	0.00	555.9	
RT 63,42,1	0.063	42,000	1	0	0.00	0.00	501.9	
RT 63,48,1	0.063	48,000	1	0	0.00	0.00	523.0	
RTP 32,42,1	0.032	42,000	1	1	0.00	0.00	412.5	
RTP 32,42,2	0.032	42,000	1	2	0.00	0.00	266.2	
RTP 32,42,3	0.032	42,000	1	3	0.00	0.00	118.3	
RTP 32,42,4	0.032	42,000	1	4	0.00	0.00	-	
RTP 32,42,5	0.032	42,000	1	5	0.00	0.00	-	
RTP 32,48,1	0.032	48,000	1	1	0.00	0.00	445.0	
RTP 32,48,2	0.032	48,000	1	2	0.00	0.00	334.1	
RTP 32,48,3	0.032	48,000	1	3	0.00	0.00	218.1	
RTP 32,48,4	0.032	48,000	1	4	0.00	0.00	72.0	
RTP 32,48,5	0.032	48,000	1	5	0.00	0.00	-	
RTP 32,48,6	0.032	48,000	1	6	0.00	0.00	-	
RTP 50,42,1	0.050	42,000	1	1	0.00	0.00	438.0	
RTP 50,42,2	0.050	42,000	1	2	0.00	0.00	360.7	
RTP 50,42,3	0.050	42,000	1	3	0.00	0.00	277.8	
RTP 50,42,4	0.050	42,000	1	4	0.00	0.00	187.8	
RTP 50,42,5	0.050	42,000	1	5	0.00	0.00	98.2	
RTP 50,42,6	0.050	42,000	1	6	0.00	0.00	3.0	

TABLE 1 (Concl'd)

RESULTS OBTAINED WITH DNA 2048 METHODS
 2024-T3 ALUMINUM PANELS, SURE-SAFE CONDITIONS
 10.0x15.0 INCH RECTANGULAR PANELS, CLAMPED EDGES

CASE I.D.	H IN	σ_y PSI	W KT	P_1 PSI	$\Delta P_{\theta=90^\circ}$ PSI	$\Delta P_{\theta=0^\circ}$ PSI	ΔT °F	SURFACE
RTP 50,48,1	0.050	48,000	1	1	0.00	0.00	466.2	
RTP 50,48,2	0.050	48,000	1	2	0.00	0.00	400.2	
RTP 50,48,3	0.050	48,000	1	3	0.00	0.00	337.4	
RTP 50,48,4	0.050	48,000	1	4	0.00	0.00	270.7	
RTP 50,48,5	0.050	48,000	1	5	0.00	0.00	196.1	
RTP 50,48,6	0.050	48,000	1	6	0.00	0.00	114.7	
RTP 63,42,1	0.063	42,000	1	1	0.00	0.00	438.5	
RTP 63,42,2	0.063	42,000	1	2	0.00	0.00	379.8	
RTP 63,42,3	0.063	42,000	1	3	0.00	0.00	322.0	
RTP 63,42,4	0.063	42,000	1	4	0.00	0.00	254.5	
RTP 63,42,5	0.063	42,000	1	5	0.00	0.00	185.4	
RTP 63,42,6	0.063	42,000	1	6	0.00	0.00	115.5	
RTP 63,48,1	0.063	48,000	1	1	0.00	0.00	465.5	
RTP 63,48,2	0.063	48,000	1	2	0.00	0.00	418.1	
RTP 63,48,3	0.063	48,000	1	3	0.00	0.00	371.1	
RTP 63,48,4	0.063	48,000	1	4	0.00	0.00	320.0	
RTP 63,48,5	0.063	48,000	1	5	0.00	0.00	264.7	
RTP 63,48,6	0.063	48,000	1	6	0.00	0.00	207.6	
RTO 32,48,0.1	0.032	48,000	0.1	0	1.16	-	24.2	
RTO 32,48,1	0.032	48,000	1	0	1.12	-	47.4	
RTO 32,48,10	0.032	48,000	10	0	1.04	-	86.7	
RTO 32,48,100	0.032	48,000	100	0	0.96	-	138.5	
RTO 32,48,1000	0.032	48,000	1,000	0	0.88	-	181.7	
RTO 50,48,1	0.050	48,000	1	0	1.73	-	59.2	
RTO 50,48,1000	0.050	48,000	1,000	0	1.22	-	224.6	
RTO 63,48,1	0.063	48,000	1	0	2.11	-	62.7	
RTO 63,48,1000	0.063	48,000	1,000	0	1.42	-	236.9	
RTO 32,48,1,P	0.032	48,000	1	0	1.15	-	27.9	POLISHED
RTO 32,48,1,NA	0.032	48,000	1	0	1.21	-	0.0	NON-ABS.
RTO 32,42,1,NA	0.032	42,000	1	0	0.99	-	0.0	NON-ABS.
RTO 50,48,1,NA	0.050	48,000	1	0	1.91	-	0.0	NON-ABS.
RTO 63,48,1,NA	0.063	48,000	1	0	2.34	-	0.0	NON-ABS.
RTO 32,42,1000	0.032	42,000	1,000	0	0.77	-	141.8	
RTO 50,42,1000	0.050	42,000	1,000	0	1.08	-	177.2	
RTO 63,42,1000	0.063	42,000	1,000	0	1.27	-	190.2	

TABLE 2

RESULTS OBTAINED WITH DNA 2048 METHODS
 2024-T3 ALUMINUM PANELS, SURE-SAFE CONDITIONS
 15.0x15.0 INCH SQUARE PANELS, CLAMPED EDGES

CASE I.D.	H IN	σ_y PSI	W KT	P _i PSI	$\Delta P_{\theta=90^\circ}$ PSI	$\Delta P_{\theta=0^\circ}$ PSI	ΔT °F	SURFACE
SO 50,42,1	0.050	42,000	1	0	1.52	2.83	0.0	
SO 50,42,1000	0.050	42,000	1,000	0	1.52	2.83	0.0	
SO 50,48,1	0.050	48,000	1	0	1.84	3.43	0.0	
SO 50,50,1	0.050	50,000	1	0	1.95	3.64	0.0	
SO 63,42,1	0.063	42,000	1	0	1.96	3.71	0.0	
SO 63,48,1	0.063	48,000	1	0	2.36	4.48	0.0	
SO 72,42,1	0.072	42,000	1	0	2.26	4.33	0.0	
SO 72,48,1	0.072	48,000	1	0	2.73	5.24	0.0	
ST 50,42,1	0.050	42,000	1	0	0.00	0.00	595.5	
ST 50,42,1000	0.050	42,000	1,000	0	0.00	0.00	595.5	
ST 50,48,1	0.050	48,000	1	0	0.00	0.00	617.8	
ST 50,50,1	0.050	50,000	1	0	0.00	0.00	624.6	
ST 63,42,1	0.063	42,000	1	0	0.00	0.00	560.2	
ST 63,48,1	0.063	48,000	1	0	0.00	0.00	582.4	
ST 72,42,1	0.072	42,000	1	0	0.00	0.00	538.8	
ST 72,48,1	0.072	48,000	1	0	0.00	0.00	562.0	
STP 50,42,1	0.050	42,000	1	1	0.00	0.00	452.7	
STP 50,42,2	0.050	42,000	1	2	0.00	0.00	368.2	
STP 50,42,3	0.050	42,000	1	3	0.00	0.00	273.8	
STP 50,42,4	0.050	42,000	1	4	0.00	0.00	175.9	
STP 50,42,5	0.050	42,000	1	5	0.00	0.00	67.1	
STP 50,48,1	0.050	48,000	1	1	0.00	0.00	480.5	
STP 50,48,2	0.050	48,000	1	2	0.00	0.00	410.1	
STP 50,48,3	0.050	48,000	1	3	0.00	0.00	334.4	
STP 50,48,4	0.050	48,000	1	4	0.00	0.00	256.5	
STP 50,48,5	0.050	48,000	1	5	0.00	0.00	177.9	
STP 50,48,6	0.050	48,000	1	6	0.00	0.00	80.3	
STP 63,42,1	0.063	42,000	1	1	0.00	0.00	460.4	
STP 63,42,2	0.063	42,000	1	2	0.00	0.00	396.2	
STP 63,42,3	0.063	42,000	1	3	0.00	0.00	336.9	
STP 63,42,4	0.063	42,000	1	4	0.00	0.00	270.5	
STP 63,42,5	0.063	42,000	1	5	0.00	0.00	196.5	
STP 63,42,6	0.063	42,000	1	6	0.00	0.00	114.8	
STP 63,48,1	0.063	48,000	1	1	0.00	0.00	486.5	
STP 63,48,2	0.063	48,000	1	2	0.00	0.00	431.5	
STP 63,48,3	0.063	48,000	1	3	0.00	0.00	383.7	

TABLE 2 (Concl'd)

RESULTS OBTAINED WITH DNA 2048 METHODS
 2024-T3 ALUMINUM PANELS, SURE-SAFE CONDITIONS
 15.0x15.0 INCH SQUARE PANELS, CLAMPED EDGES

CASE I.D.	H IN	σ_y PSI	W KT	P _i PSI	$\Delta P_{\theta=90^\circ}$ PSI	$\Delta P_{\theta=0^\circ}$ PSI	ΔT °F	SURFACE
STP 63,48,4	0.063	48,000	1	4	0.00	0.00	333.3	
STP 63,48,5	0.063	48,000	1	5	0.00	0.00	277.8	
STP 63,48,6	0.063	48,000	1	6	0.00	0.00	212.8	
STP 72,42,1	0.072	42,000	1	1	0.00	0.00	462.4	
STP 72,42,2	0.072	42,000	1	2	0.00	0.00	401.9	
STP 72,42,3	0.072	42,000	1	3	0.00	0.00	348.4	
STP 72,42,4	0.072	42,000	1	4	0.00	0.00	296.8	
STP 72,42,5	0.072	42,000	1	5	0.00	0.00	238.2	
STP 72,42,6	0.072	42,000	1	6	0.00	0.00	176.5	
STP 72,48,1	0.072	48,000	1	1	0.00	0.00	487.6	
STP 72,48,2	0.072	48,000	1	2	0.00	0.00	436.3	
STP 72,48,3	0.072	48,000	1	3	0.00	0.00	392.1	
STP 72,48,4	0.072	48,000	1	4	0.00	0.00	352.1	
STP 72,48,5	0.072	48,000	1	5	0.00	0.00	309.6	
STP 72,48,6	0.072	48,000	1	6	0.00	0.00	261.4	
STO 50,48,0.1	0.050	48,000	0.1	0	1.77	-	21.5	
STO 50,48,1	0.050	48,000	1	0	1.71	-	43.0	
STO 50,48,10	0.050	48,000	10	0	1.61	-	81.2	
STO 50,48,100	0.050	48,000	100	0	1.46	-	140.8	
STO 50,48,1000	0.050	48,000	1000	0	1.26	-	207.5	
STO 63,48,1	0.063	48,000	1	0	2.17	-	48.4	
STO 63,48,1000	0.063	48,000	1000	0	1.55	-	232.4	
STO 72,48,1	0.072	48,000	1	0	2.51	-	54.0	
STO 72,48,1000	0.072	48,000	1000	0	1.72	-	239.5	
STO 50,48,1,P	0.050	48,000	1	0	1.75	-	25.0	POLISHED
STO 50,48,1,NA	0.050	48,000	1	0	1.84	-	0.0	NON-ABS.
STO 50,42,1,NA	0.050	42,000	1	0	1.52	-	0.0	NON-ABS.
STO 63,48,1,NA	0.063	48,000	1	0	2.34	-	0.0	NON-ABS.
STO 72,48,1,NA	0.072	48,000	1	0	2.73	-	0.0	NON-ABS.
STO 50,42,1000	0.050	42,000	1000	0	1.10	-	166.7	
STO 63,42,1000	0.063	42,000	1000	0	1.37	-	189.7	
STO 72,42,1000	0.072	42,000	1000	0	1.51	-	195.5	

TABLE 3

RESULTS OBTAINED WITH DNA 2048 DEPROB METHOD
 2024-T3 ALUMINUM, ELASTIC/PLASTIC RESPONSE
 10.0 INCH LONG CLAMPED BEAM ELEMENT FROM RECTANGULAR PANEL

CASE I.D.	H IN	σ_y PSI	$\Delta P_{\theta=90^\circ}$ PSI	$\Delta P_{\theta=0^\circ}$ PSI	$\Delta P_{y\theta=0^\circ}$ PSI	$w_{\text{cent peak}}$ IN	$t_{w_{cp}}$ MSEC	$t_{\text{edge yield}}$ MSEC
BRDI 32,42,25.3	0.032	42,000	10	25.3	1.43			
					1.51	0.198	1.60	1.766
BRDI 32,42,11.4	0.032	42,000	5	11.4	1.44			
					1.57	0.201	1.55	1.710
BRDI 32,42,6.5	0.032	42,000	3	6.5	1.45			
					1.59	0.202	1.55	1.696
BRDI 32,42,2.0	0.032	42,000	1	2.0	1.42			
					1.46	0.196	1.60	1.822
BRDI 32,50,25.3	0.032	50,000	10	25.3	1.95			
					2.25	0.229	1.35	1.268
BRDI 32,48,2.0	0.032	48,000	1	2.0	1.55			
					1.54	0.200	1.55	(NO YIELD)
BRDI 50,48,2.0	0.050	48,000	1	2.0	2.37			
					2.27	0.182	1.55	(NO YIELD)
BRD 32,42,25.3	0.032	42,000	10	25.3	-	0.605	0.70	0.158
BRD 32,42,11.4	0.032	42,000	5	11.4	-	0.419	0.82	0.328
BRD 32,42,6.5	0.032	42,000	3	6.5	-	0.340	1.00	0.494
BRD 32,42,2.0	0.032	42,000	1	2.0	-	0.220	1.45	1.230
BRD 32,48,2.0	0.032	48,000	1	2.0	-	0.220	1.45	1.354
BRD 50,48,2.0	0.050	48,000	1	2.0	-	0.173	1.65	(NO YIELD)
BRS 32,42,2	0.032	42,000	-	2	-	0.132	-	-
BRS 32,42,3	0.032	42,000	-	3	-	0.152	-	-
BRS 32,42,4	0.032	42,000	-	4	-	0.168	-	-
BRS 32,48,2	0.032	48,000	-	2	-	0.132	-	-
BRS 50,48,2	0.050	48,000	-	2	-	0.107	-	-
BRS 50,48,3	0.050	48,000	-	3	-	0.125	-	-

TABLE 4

EXPERIMENTS ON 2024-T3 ALUMINUM PANELS, CLAMPED EDGES
 15.0x15.0x0.050 IN. OR 10.0x15.0x0.032 IN. EXPOSED SIZE

NSWC TEST #	KA TEST #	PANEL W x H (in)	PINT (PSI)	ΔT (°F)	ΔP_B (PSI)	MOUNT	GAGES ON SURFACE
9A	1	15x15	2	0	0	INSULATED	SG, IN&OUT
9B	2	↓	4	↓	↓	↓	↓
10A	1	↓	2	↓	↓	↓	↓
10B	2	↓	4	↓	↓	↓	↓
11A	4	↓	2	↓	↓	-	↓
11B	5	↓	4	↓	↓	-	↓
12A	4	↓	2	↓	↓	-	↓
12B	5	↓	4	↓	↓	-	↓
13A	7	↓	2	↓	↓	INVERTED	↓
13B	8	↓	4	↓	↓	↓	↓
14A	7	↓	2	↓	↓	↓	↓
14B	8	↓	4	↓	↓	↓	↓
15A	13	10x15	2	↓	↓	INSULATED	↓
15B	14	↓	4	↓	↓	↓	↓
16A	13	↓	2	↓	↓	↓	↓
16B	14	↓	4	↓	↓	↓	↓
17A	16	↓	2	↓	↓	-	↓
17B	17	↓	4	↓	↓	-	↓
18A	16	↓	2	↓	↓	-	↓
18B	17	↓	4	↓	↓	-	↓
19A	19	↓	2	↓	↓	INVERTED	↓
19B	20	↓	4	↓	↓	↓	↓
20A	19	↓	2	↓	↓	↓	↓
20B	20	↓	4	↓	↓	↓	↓
21	3	10x15	0	0	1.65	INVERTED	SG, IN, X&Y
22	6	↓	↓	↓	1.51	INSULATED	↓
23	9	↓	↓	↓	1.78	-	↓
24	10	↓	↓	↓	2.92	-	↓
25	11	↓	↓	↓	4.21	-	↓
26	12	↓	↓	↓	5.14	-	↓
27	-	↓	↓	↓	6.61	-	↓
28	-	↓	↓	↓	7.62	-	↓
29	-	↓	↓	↓	8.92	-	↓
30	-	↓	↓	↓	10.17	-	↓
31	-	↓	↓	↓	-	-	↓
32	-	↓	↓	↓	12.57	-	↓
33	-	↓	↓	↓	13.98	-	↓
34	15	15x15	↓	↓	2.14	INVERTED	↓
35	18	↓	↓	↓	-	INSULATED	↓
36	21	↓	↓	↓	2.20	INSULATED	↓
37	22	↓	↓	↓	2.29	-	↓

TABLE 4 (Cont'd)

EXPERIMENTS ON 2024-T3 ALUMINUM PANELS, CLAMPED EDGES
15.0x15.0x0.050 IN. OR 10.0x15.0x0.032 IN. EXPOSED SIZE

NSWC TEST #	KA TEST #	PANEL W x H (in)	PINT (PSI)	ΔT (°F)	ΔP_B (PSI)	MOUNT	GAGES ON SURFACE
38	23	15x15	0	0	4.90	-	SG, IN, X&Y
39	-	↓	↓	↓	6.72	-	↓
40	-	↓	↓	↓	8.16	-	↓
41	-	↓	↓	↓	11.12	-	↓
42	-	↓	↓	↓	13.22	-	↓
55	-	15x15	0	0	1.7	-	SG, IN&OUT
58	-	↓	↓	↓	3.1	-	↓
59	-	↓	↓	↓	4.0	-	↓
60	-	↓	↓	↓	5.6	-	↓
62	-	15x15	0	320	1.3	INSULATED	SG, TC, IN
63	-	↓	↓	291	3.2	↓	↓
64	-	↓	↓	265	4.2	↓	↓
65	-	15x15	0	MAX 500	NO BLAST	INSULATED	SG, TC, IN
66	-	↓	↓	MAX 300	1.3	↓	↓
67	-	↓	↓	MAX 300	3.0	↓	↓
68	-	↓	↓	MAX 400	1.35	↓	↓
69	-	↓	↓	MAX 400	4.35	↓	↓
70	-	↓	↓	MAX 350	1.03	↓	↓
78	-	15x15	4.0	MAX 400	0	INSULATED	SG, TC, IN
79	-	↓	4.55	MAX 250	↓	↓	↓
80	-	↓	4.38	MAX 550	↓	↓	↓
84.1	R1.1	10x15	2	-	-	-	SG, IN&OUT
84.2	R1.2	↓	4	-	-	-	↓
85	R1.3	↓	-	-	NO RECORD	-	↓
87	S2.1	15x15	-	MAX 430	-	INSULATED	SG, TC, IN
88	S2.2	↓	-	MAX 590	-	↓	↓
89	S3	↓	-	MAX 630	-	↓	↓
91	R2.1	10x15	-	MAX 590	-	↓	↓
92	R2.2	↓	-	MAX 390	-	↓	↓
93	R3	↓	-	MAX 800	-	↓	↓
97.1	S1.1	15x15	2	-	-	-	SG, IN&OUT
97.2	S1.2	↓	4	-	-	-	↓
97.3	S1.3	↓	-	-	51.0	-	↓

TABLE 4 (Concl'd)

EXPERIMENTS ON 2024-T3 ALUMINUM PANELS, CLAMPED EDGES
 15.0x15.0x0.050 IN. OR 10.0x15.0x0.032 IN. EXPOSED SIZE

<u>NSWC</u> <u>TEST #</u>	<u>KA</u> <u>TEST #</u>	<u>PANEL</u> <u>W x H</u> <u>(in)</u>	<u>PINT</u> <u>(PSI)</u>	<u>ΔT</u> <u>($^{\circ}$F)</u>	<u>ΔP_B</u> <u>(PSI)</u>	<u>MOUNT</u>	<u>GAGES</u> <u>ON</u> <u>SURFACE</u>
99.1	R4.1	10x15	2	-	-	INSULATED	SG, TC, IN
99.2	R4.2	↓	2	MAX 402	-	↓	↓
99.3	R4.3		2	MAX 578	-		
100.1	R6.1		6	-	-		
100.2	R6.2		6	MAX 367	-		
101.1	R6.1		6	-	-		
101.2	R6.2	↓	6	MAX 407	-	↓	↓
102.1	S4.1		4	-	-		
102.2	S4.2		4	MAX 712	-		
103.1	S5.1	↓	4	-	-	↓	↓
103.2	S5.2		4	MAX 218	-		
104	S6	↓	6	MAX 331	-	↓	↓
105	R7		6	MAX 346	-		

TABLE 5

SAMPLE OVERPRESSURE DATA REDUCTION

TEST NO.	GAGE	Calibration from setup sheets		measured from traces (in)			$\Delta p \left(\frac{C_s Q_v}{\Delta c} \right)$		Δp_{mean} (PSI)	Δp_{peak} (PSI)
		C_s (pf)	Q_v (v)	ΔC	Δp_{mean}	Δp_{peak}	PKA_{mean}	PKA_{peak}		
24 (RECT)	1	100	2.0	1.78	1.26	1.31	142	147	1.50	1.55
	2	200	2.0	2.08	1.82	1.90	350	365	3.20	3.35
25 (RECT)	1	100	2.0	1.67	1.67	1.77	200	212	2.12	2.25
	2	200	2.0	2.08	2.63	2.71	506	521	4.72	4.85
29 (RECT)	1	200	2.0	1.92	1.76	1.86	367	388	4.05	4.32
	2	200	2.0	1.00	2.30	2.42	920	968	9.18	9.70
33 (RECT)	1	400	2.0	1.51	0.94	1.02	498	540	5.70	6.25
	2	500	2.0	1.21	1.68	1.77	1,388	1,463	14.55	15.45
37 (SQ)	1	100	2.0	2.89	1.26	1.34	87	93	0.91	0.97
	2	100	2.0	1.50	1.80	1.98	240	264	2.15	2.38
38 (SQ)	1	100	2.0	1.56	1.61	1.71	206	219	2.18	2.33
	2	100	2.0	1.01	2.77	3.04	549	602	5.18	5.72
39 (SQ)	1	200	2.0	1.85	1.28	1.38	277	298	2.99	3.23
	2	200	2.0	1.08	1.96	2.21	726	819	7.03	8.05
42 (SQ)	1	400	(2.0)	1.86	1.11	1.18	477	508	5.44	5.85
	2	500	(2.0)	1.50	1.98	2.13	1,320	1,420	13.75	14.95

NOTE: GAGE 1: SIDE-ON (INCIDENT) PRESSURE
 GAGE 2: FACE-ON (REFLECTED) PRESSURE

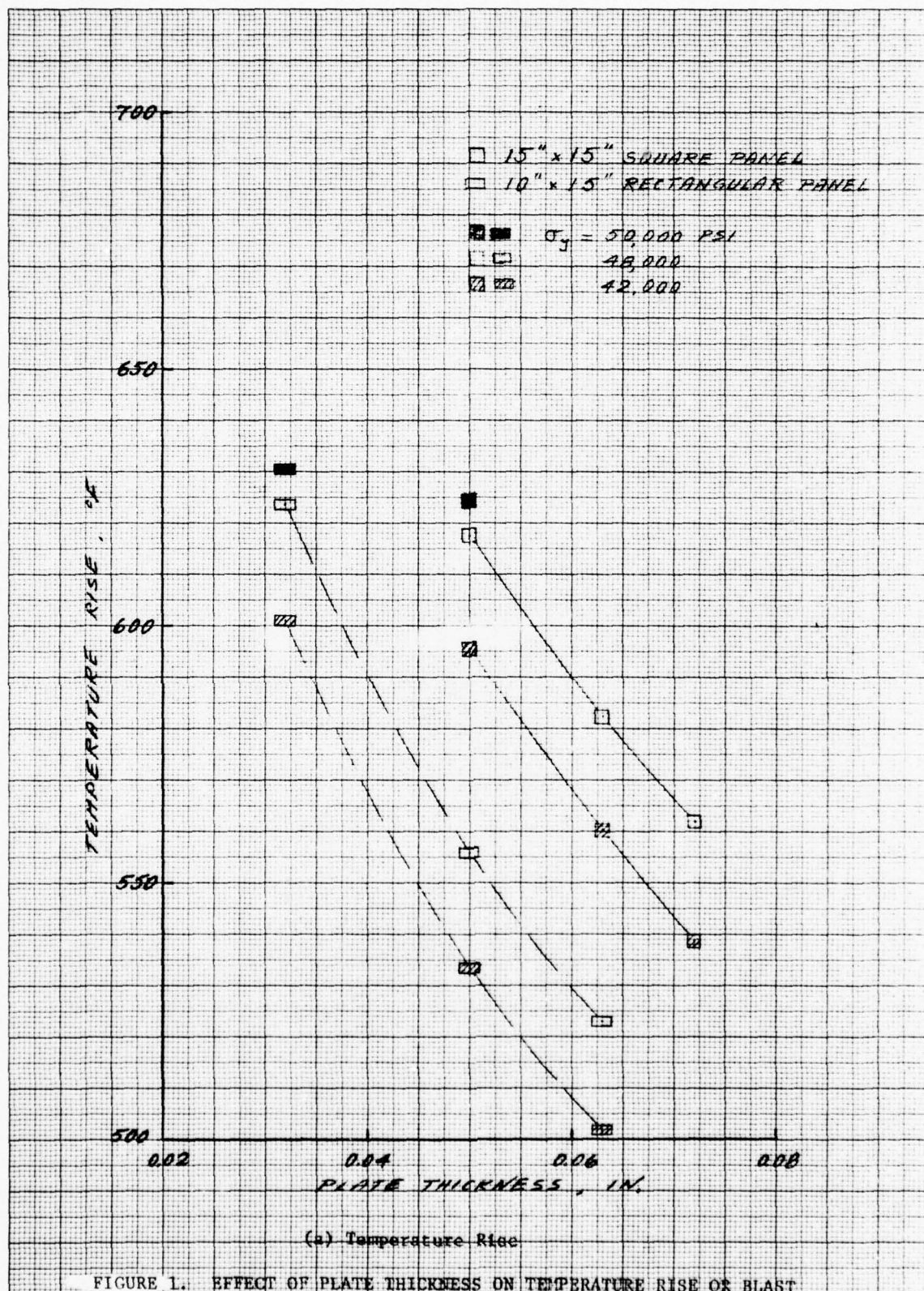
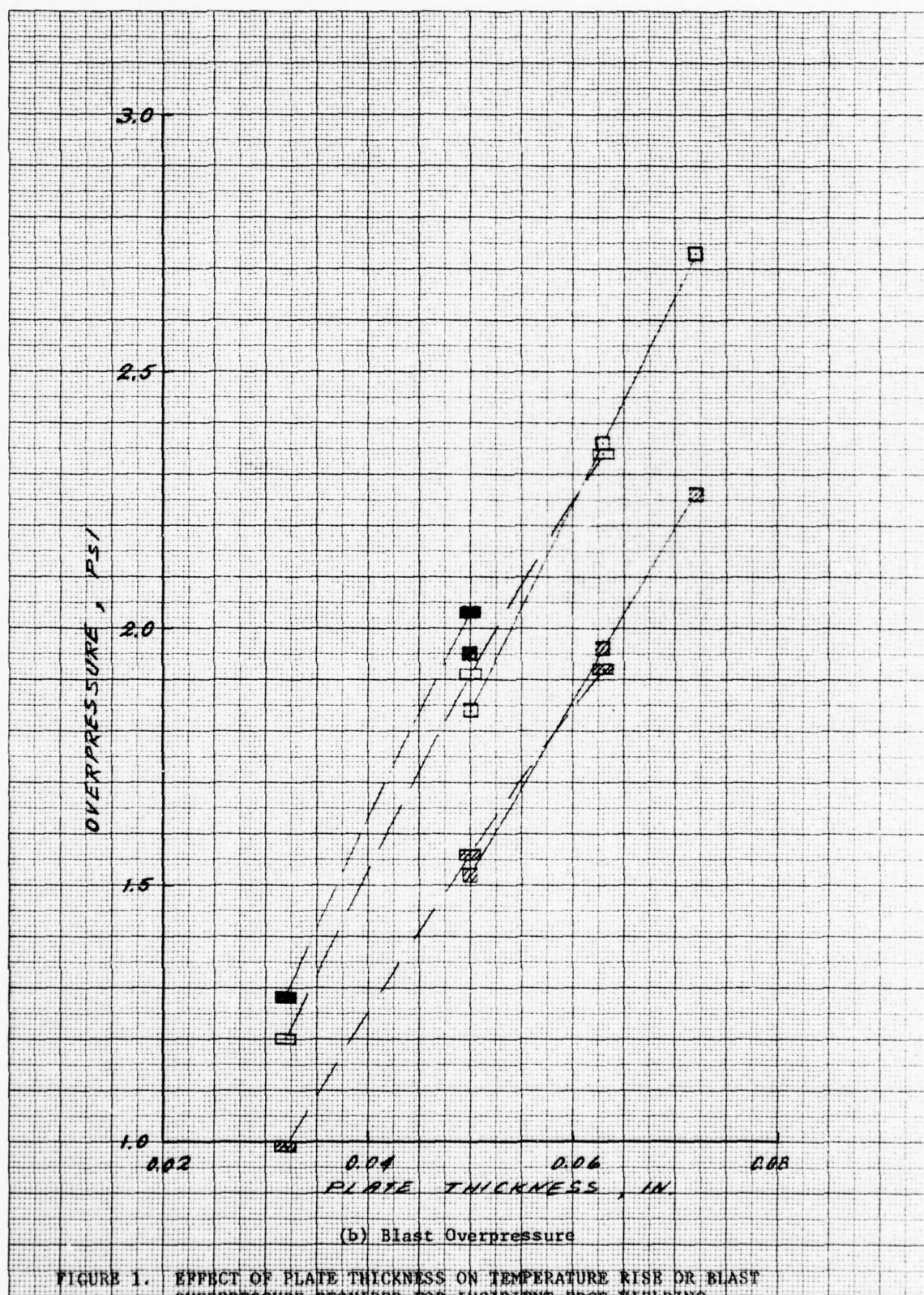


FIGURE 1. EFFECT OF PLATE THICKNESS ON TEMPERATURE RISE OF BLAST OVERPRESSURE REQUIRED FOR INCIPIENT EDGE YIELDING



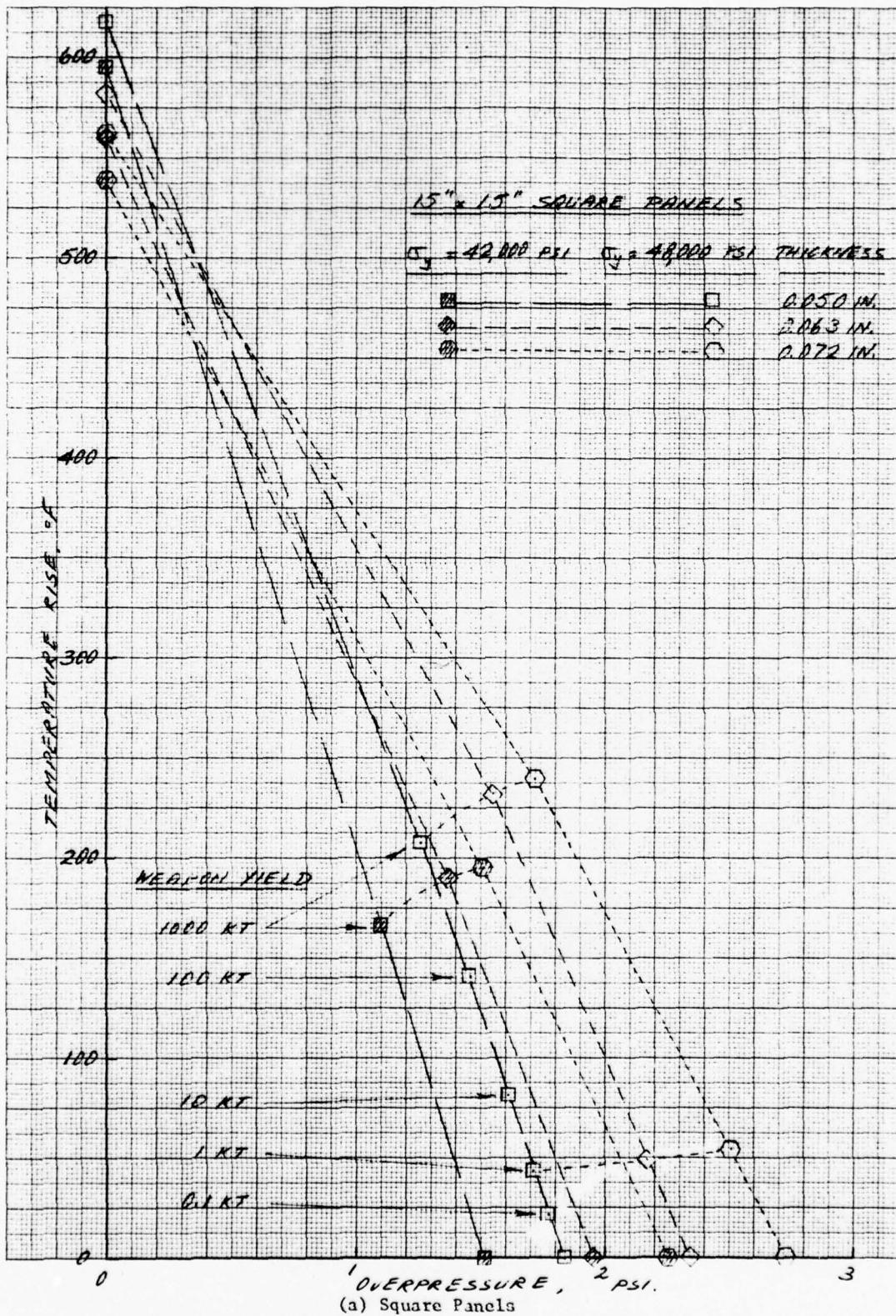
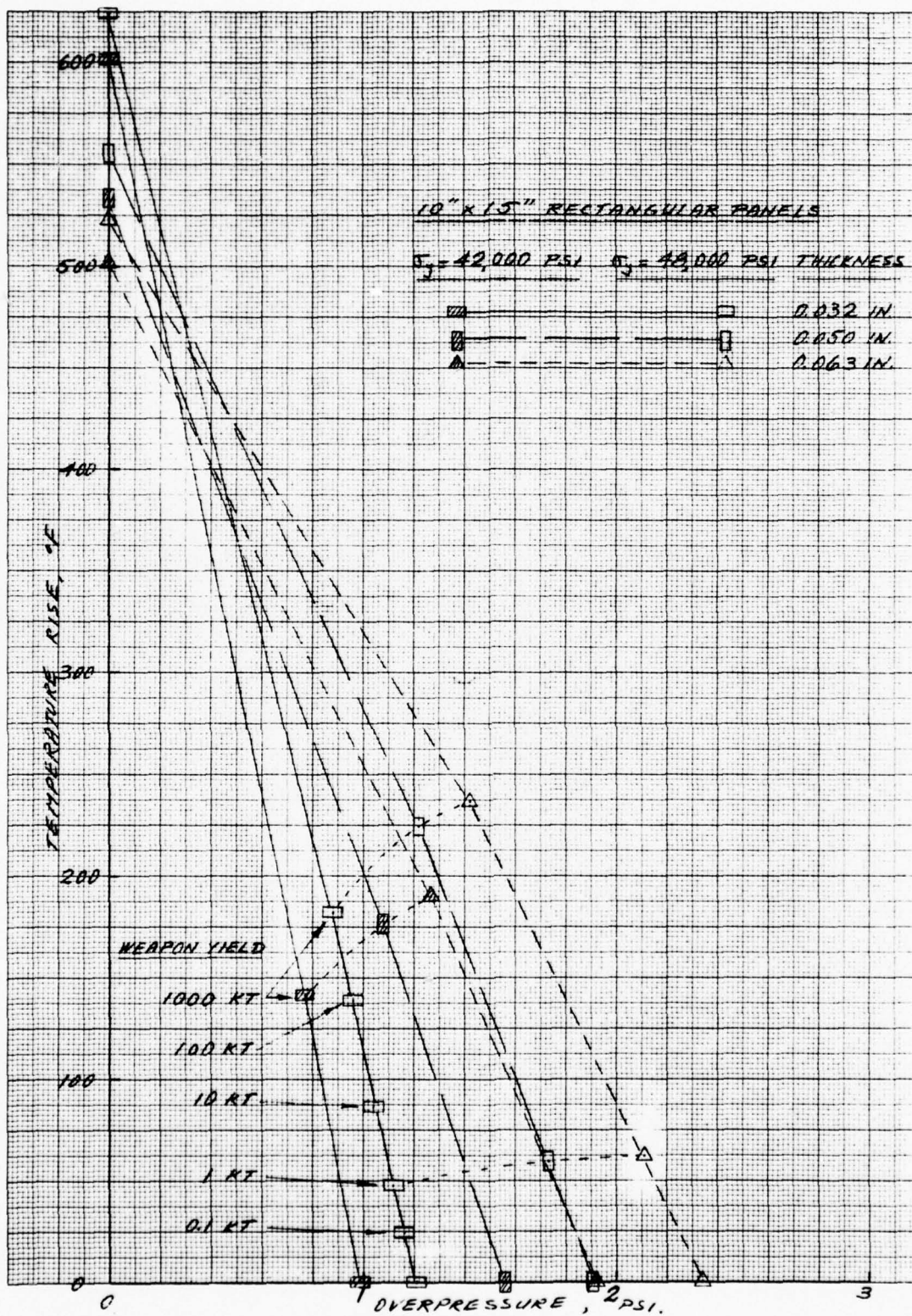
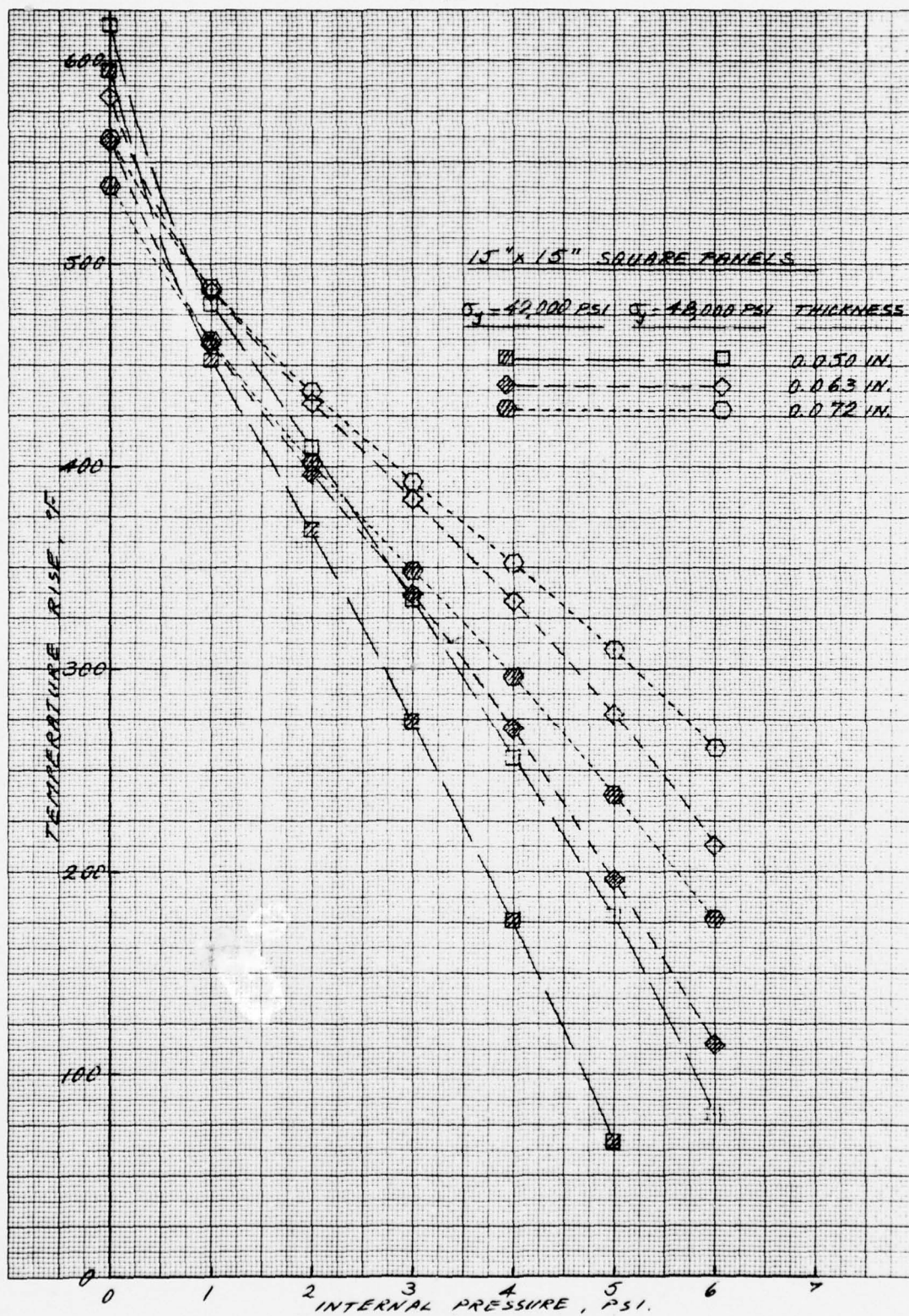


FIGURE 2. COMBINED EFFECTS OF TEMPERATURE RISE AND BLAST OVERPRESSURE REQUIRED FOR INCIPIENT EDGE YIELDING



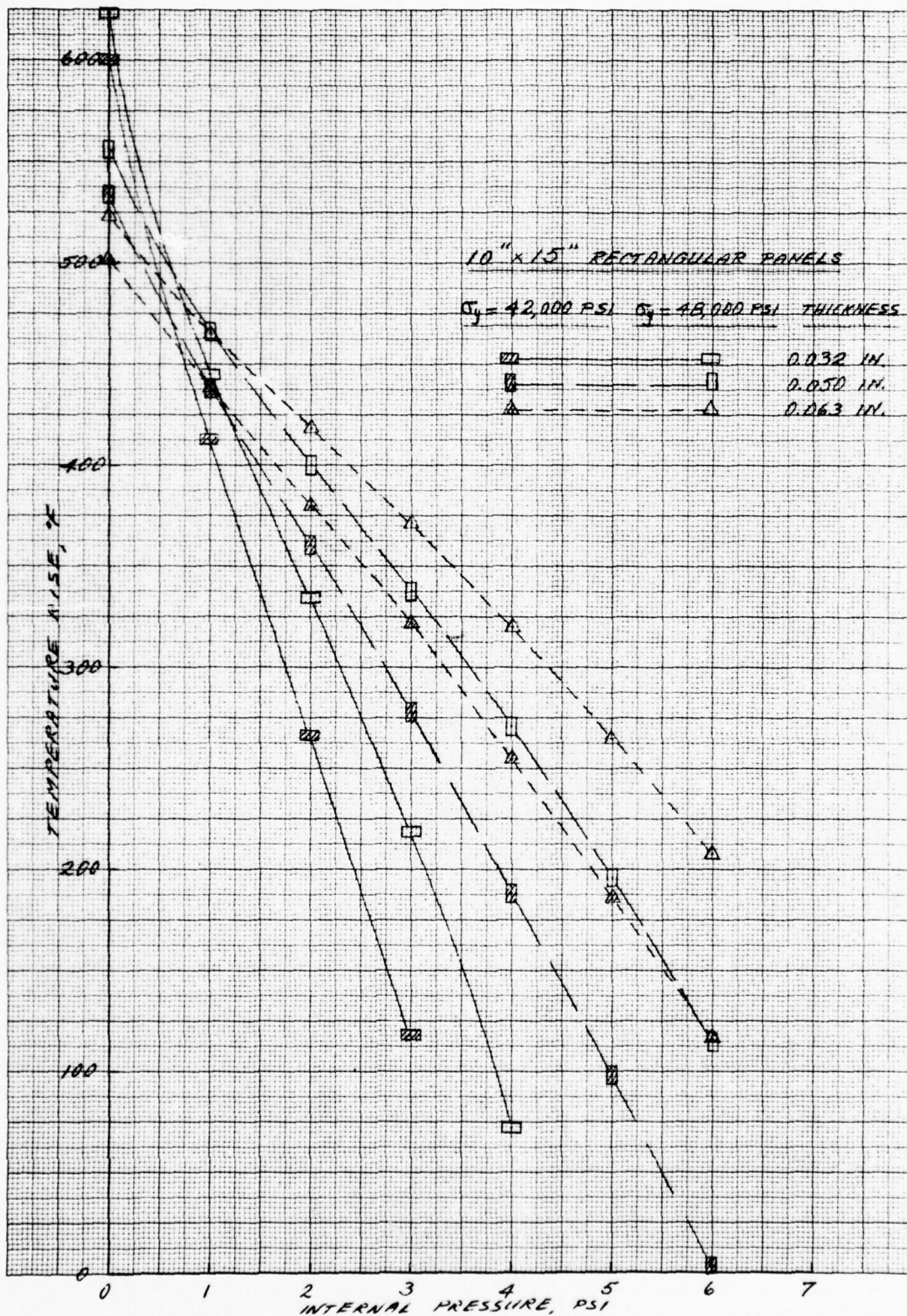
(b) Rectangular Panels

FIGURE 2. COMBINED EFFECTS OF TEMPERATURE RISE AND BLAST OVERPRESSURE REQUIRED FOR INCIPIENT EDGE YIELDING



(a) Square Panels

FIGURE 3. COMBINED EFFECTS OF TEMPERATURE RISE AND INTERNAL PRESSURIZATION REQUIRED FOR INCIPIENT EDGE YIELDING



(b) Rectangular Panels

FIGURE 3. COMBINED EFFECTS OF TEMPERATURE RISE AND INTERNAL PRESSURIZATION REQUIRED FOR INCIPIENT EDGE YIELDING

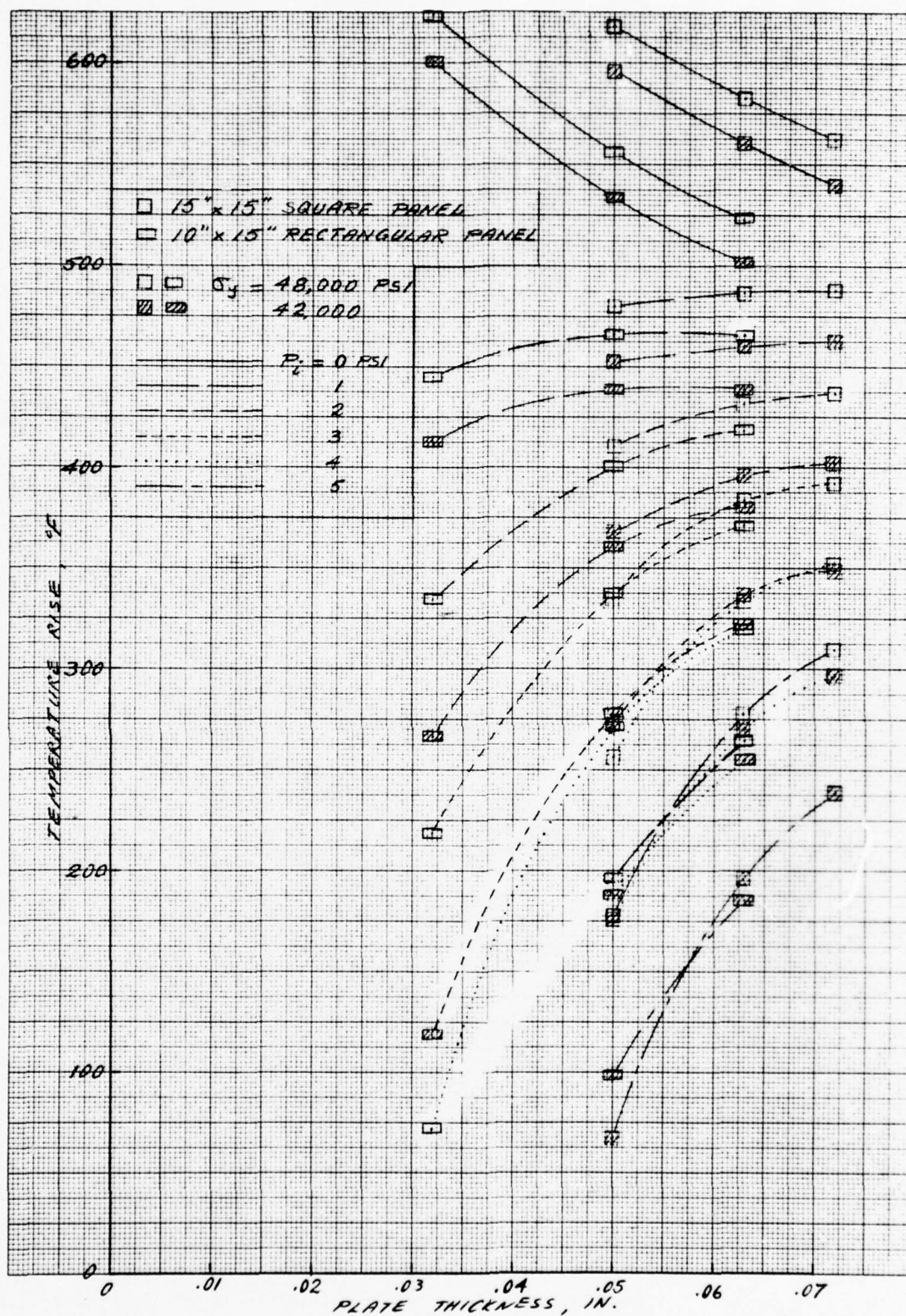
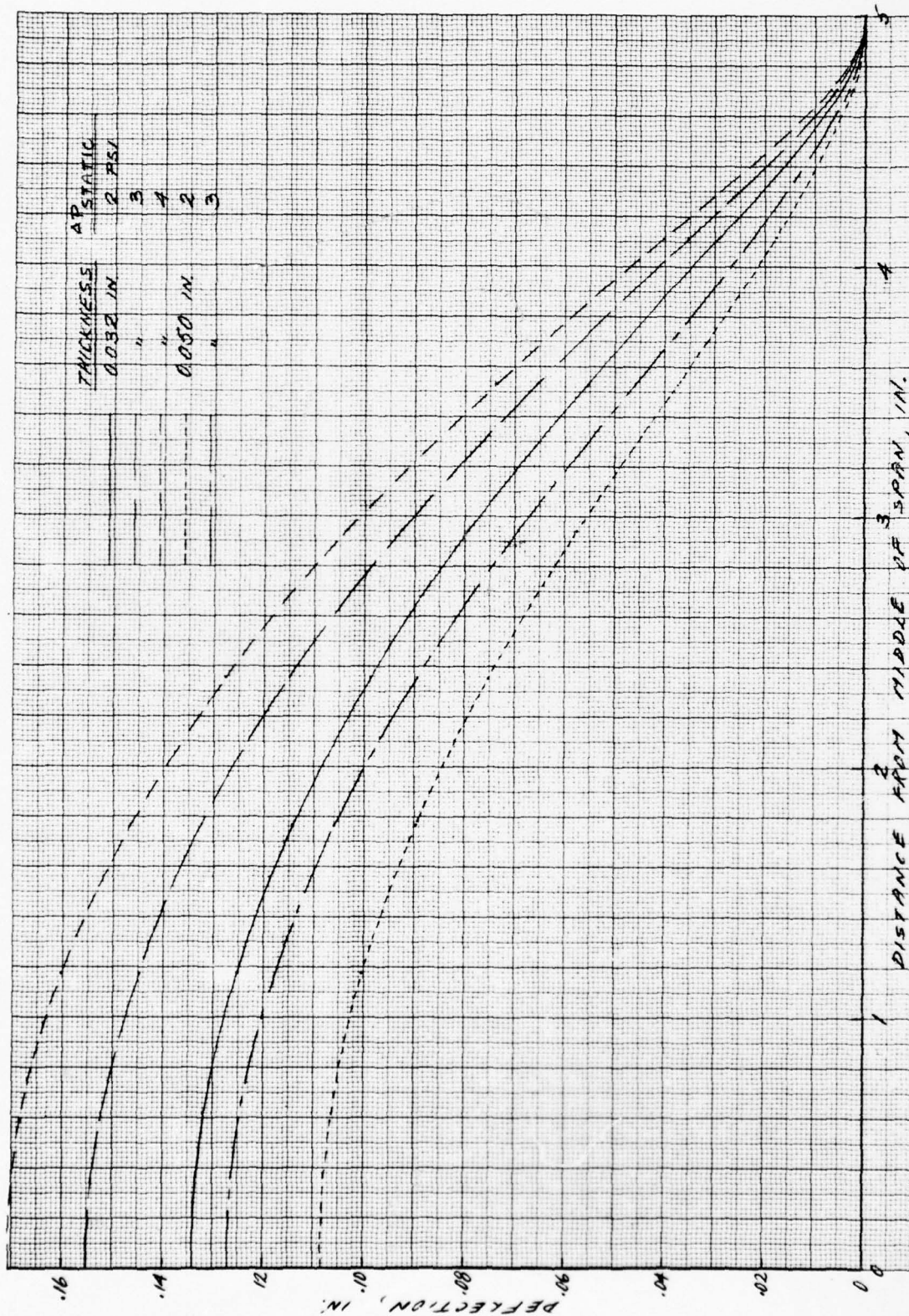
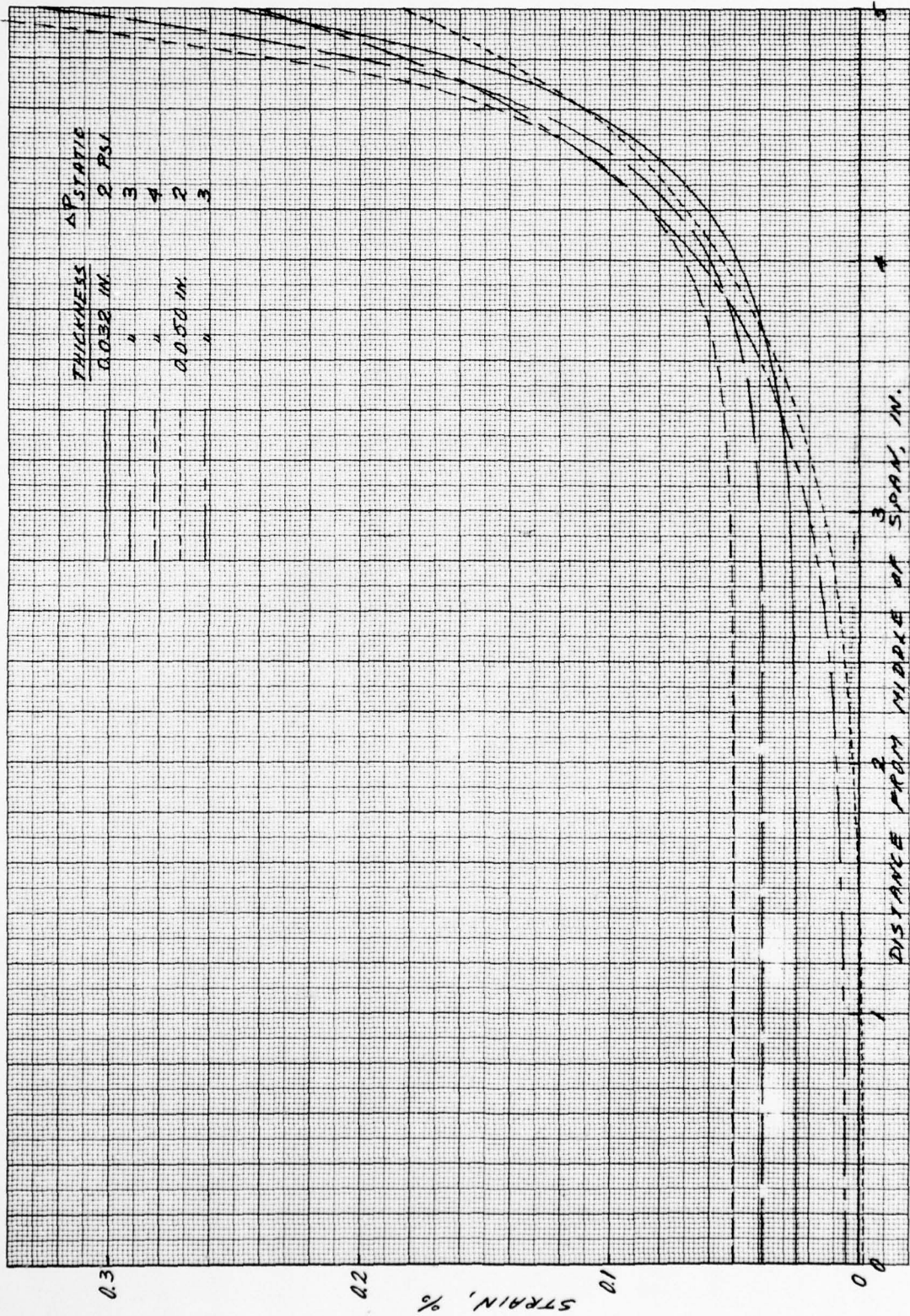


FIGURE 4. EFFECT OF PLATE THICKNESS ON THE COMBINED EFFECTS OF THERMAL/PRESSURIZATION EXPOSURE REQUIRED FOR INCIPIENT EDGE YIELDING



(a) Deflection Distribution
 FIGURE 5. DEFLECTIONS AND STRAINS OBTAINED FROM THE BEAM ELEMENT MODEL SUBJECTED TO STATIC PRESSURE



(b) Strain Distribution
 FIGURE 5. DEFLECTIONS AND STRAINS OBTAINED FROM THE BEAM ELEMENT MODEL SUBJECTED TO STATIC PRESSURE

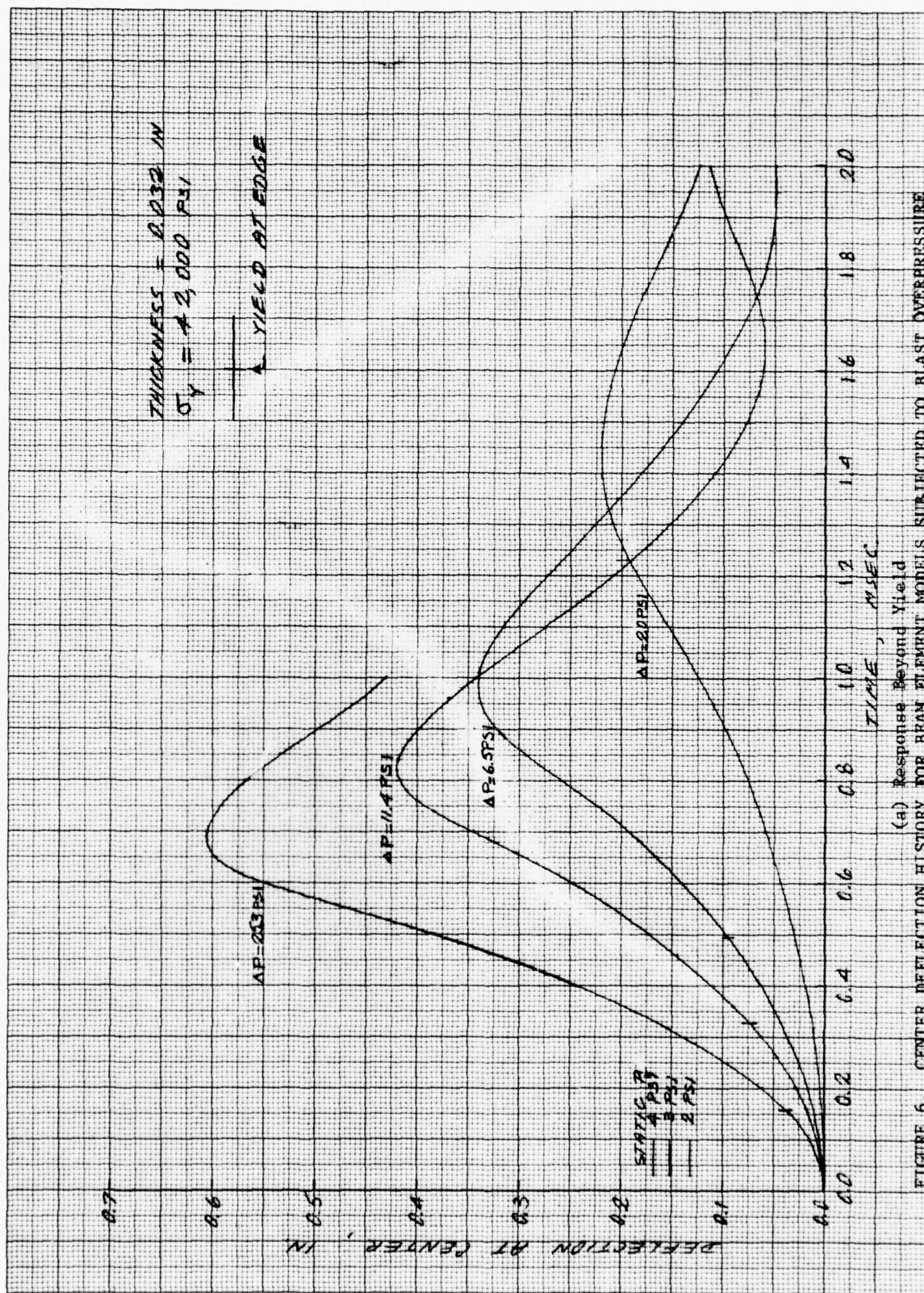


FIGURE 6. CENTER DEFLECTION HISTORY FOR BEAM ELEMENT MODELS SUBJECTED TO BLAST OVERPRESSURE

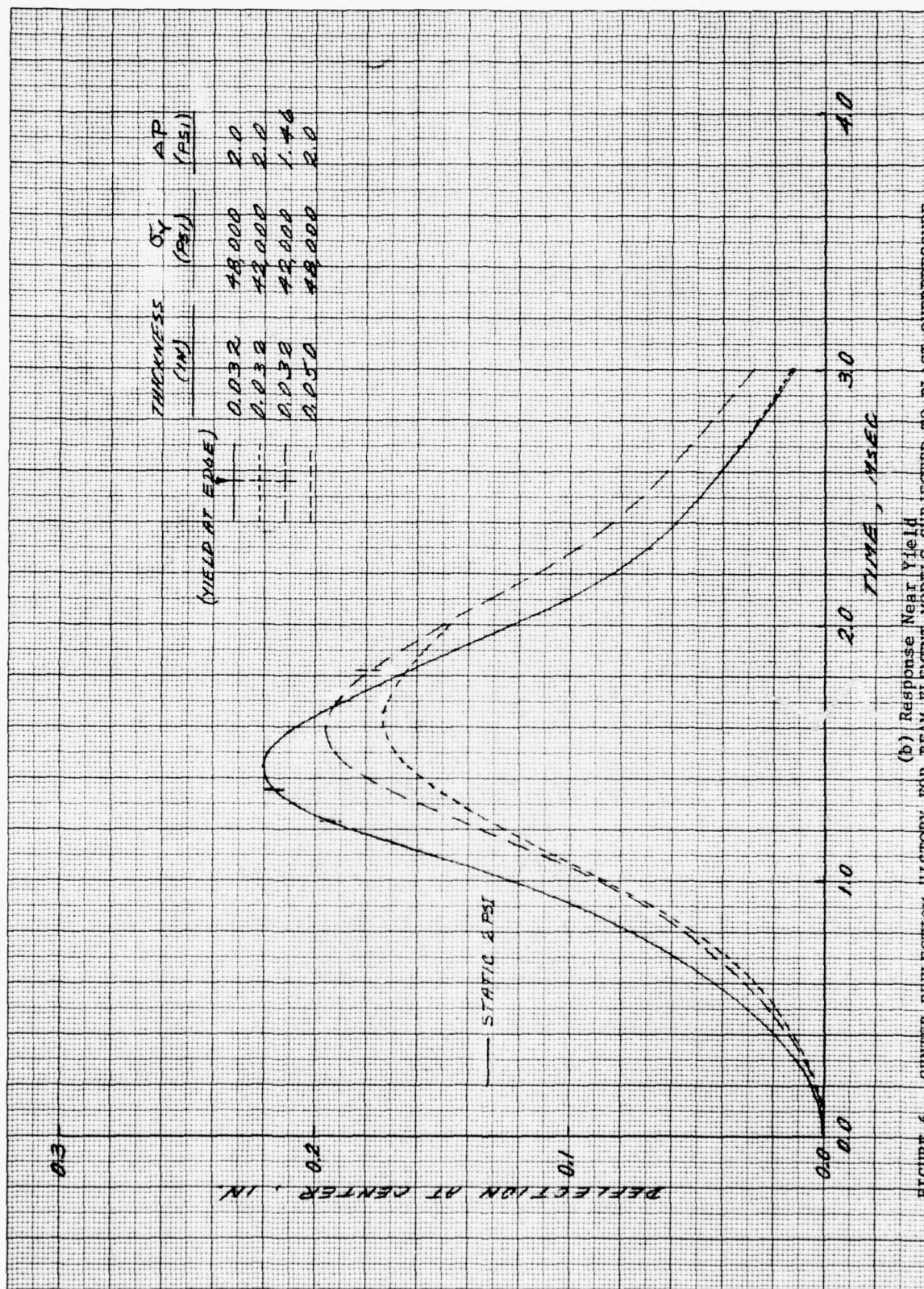


FIGURE 6. CENTER DEFLECTION HISTORY FOR BEAM ELEMENT MODELS SUBJECTED TO BLAST OVERPRESSURE
(b) Response Near Yield

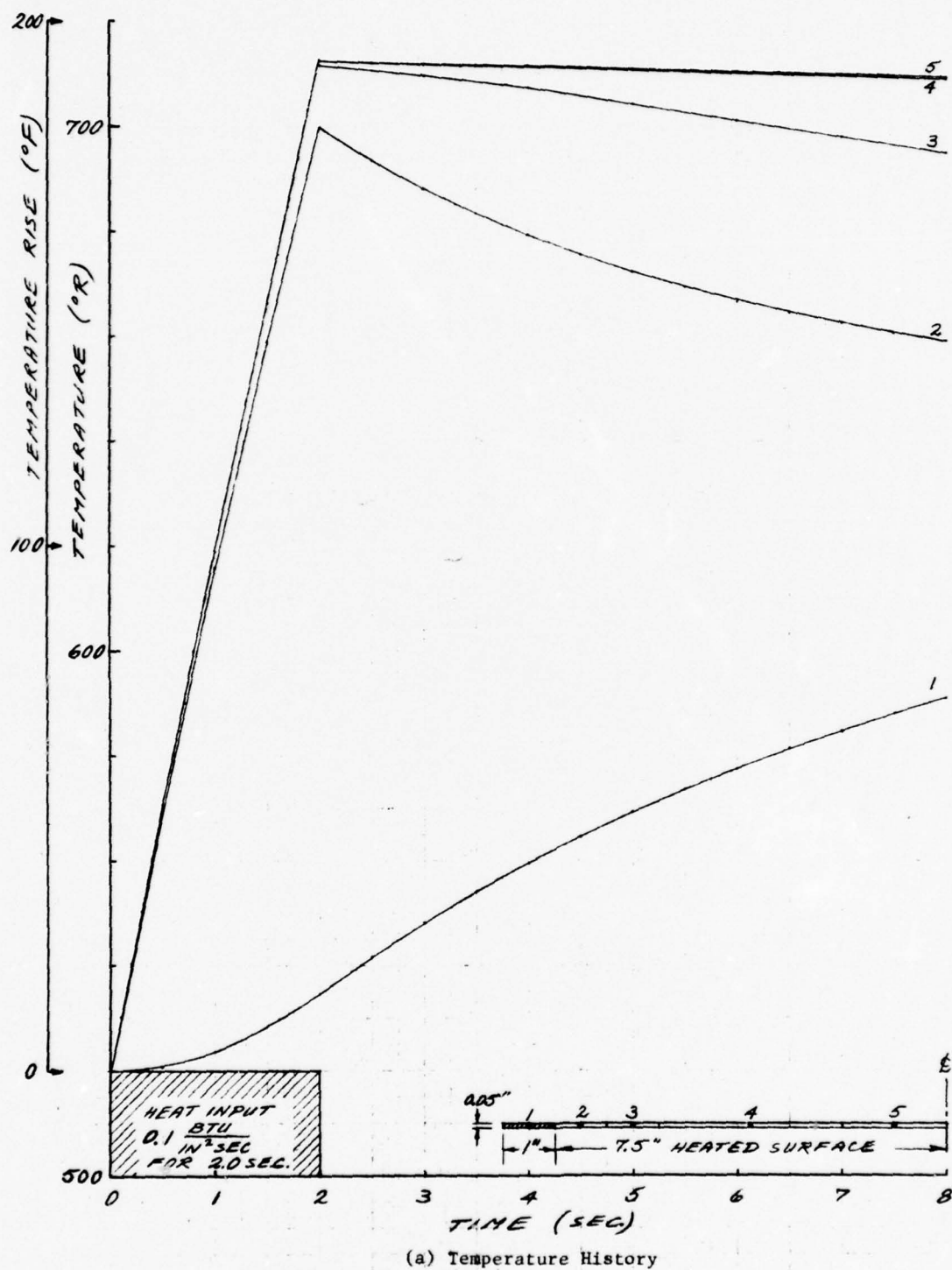
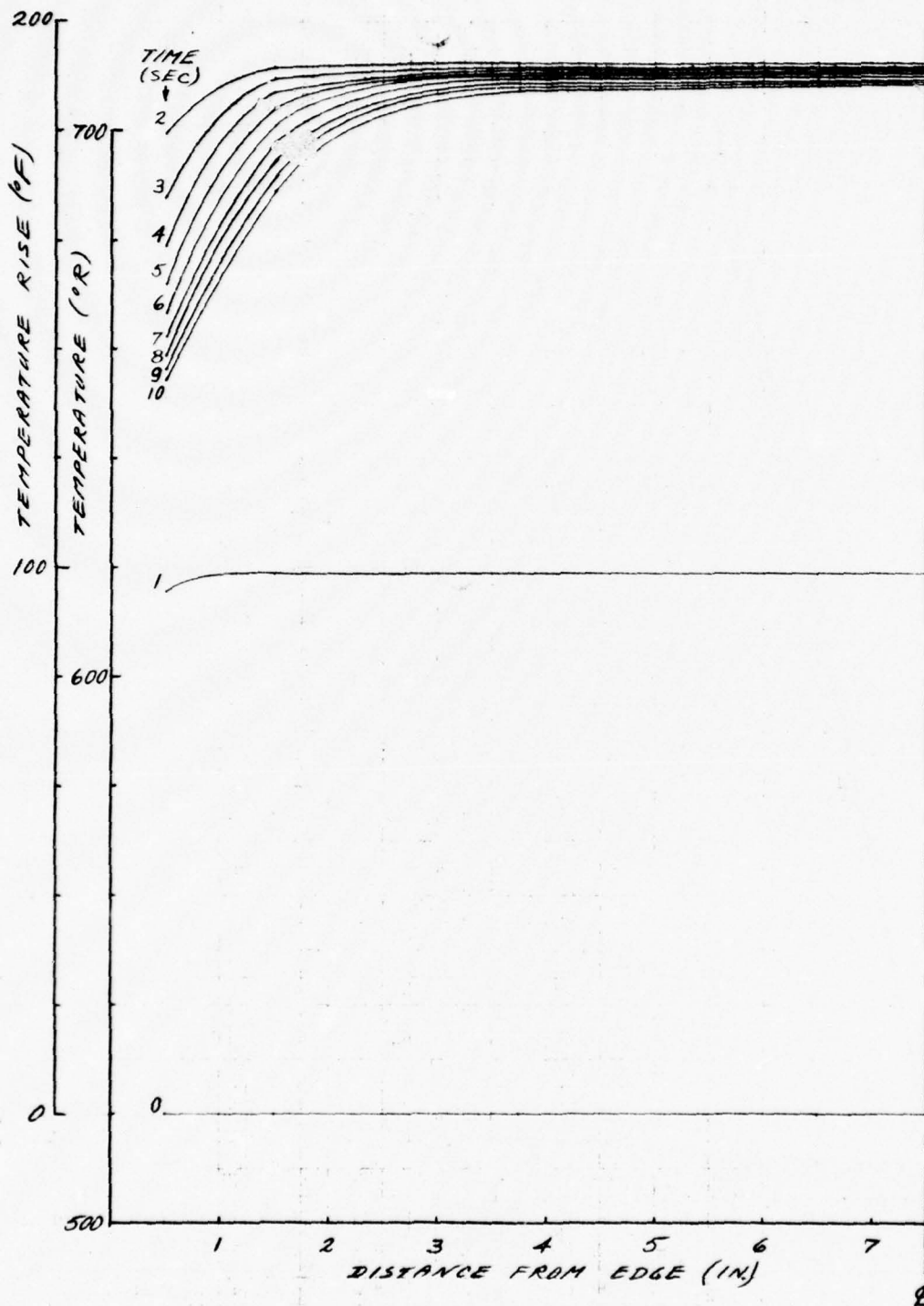


FIGURE 7. TEMPERATURE HISTORY AND DISTRIBUTION AT CENTERLINE OF SQUARE PANELS SUBJECTED TO THERMAL EXPOSURE WITH A SMALL HEAT SINK AT EDGE



(b) Temperature Distribution

FIGURE 7. TEMPERATURE HISTORY AND DISTRIBUTION AT CENTERLINE OF SQUARE PANELS SUBJECTED TO THERMAL EXPOSURE WITH A SMALL HEAT SINK AT EDGE

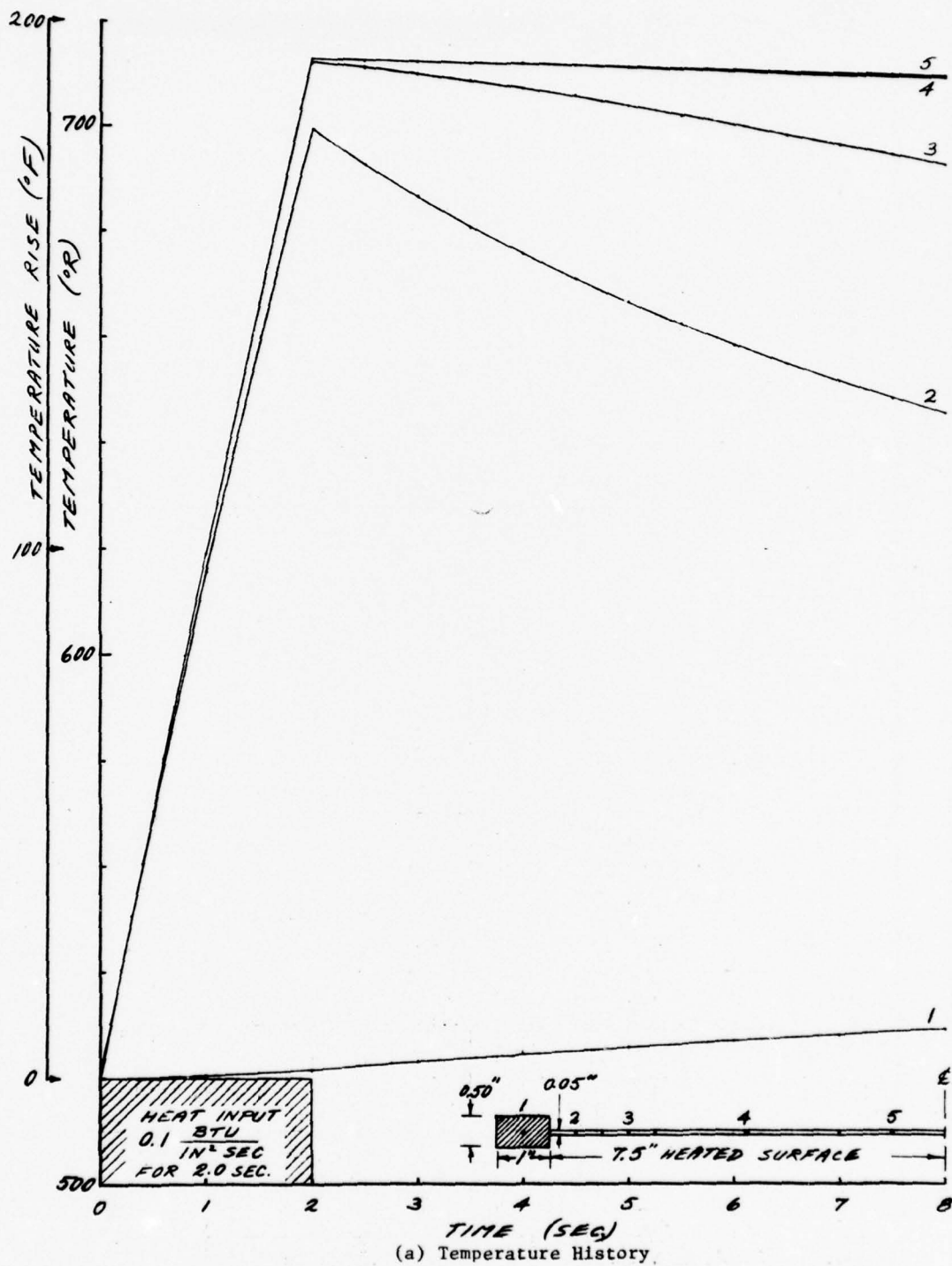


FIGURE 8. TEMPERATURE HISTORY AND DISTRIBUTION AT CENTERLINE OF SQUARE PANELS SUBJECTED TO THERMAL EXPOSURE WITH A LARGE HEAT SINK AT EDGE

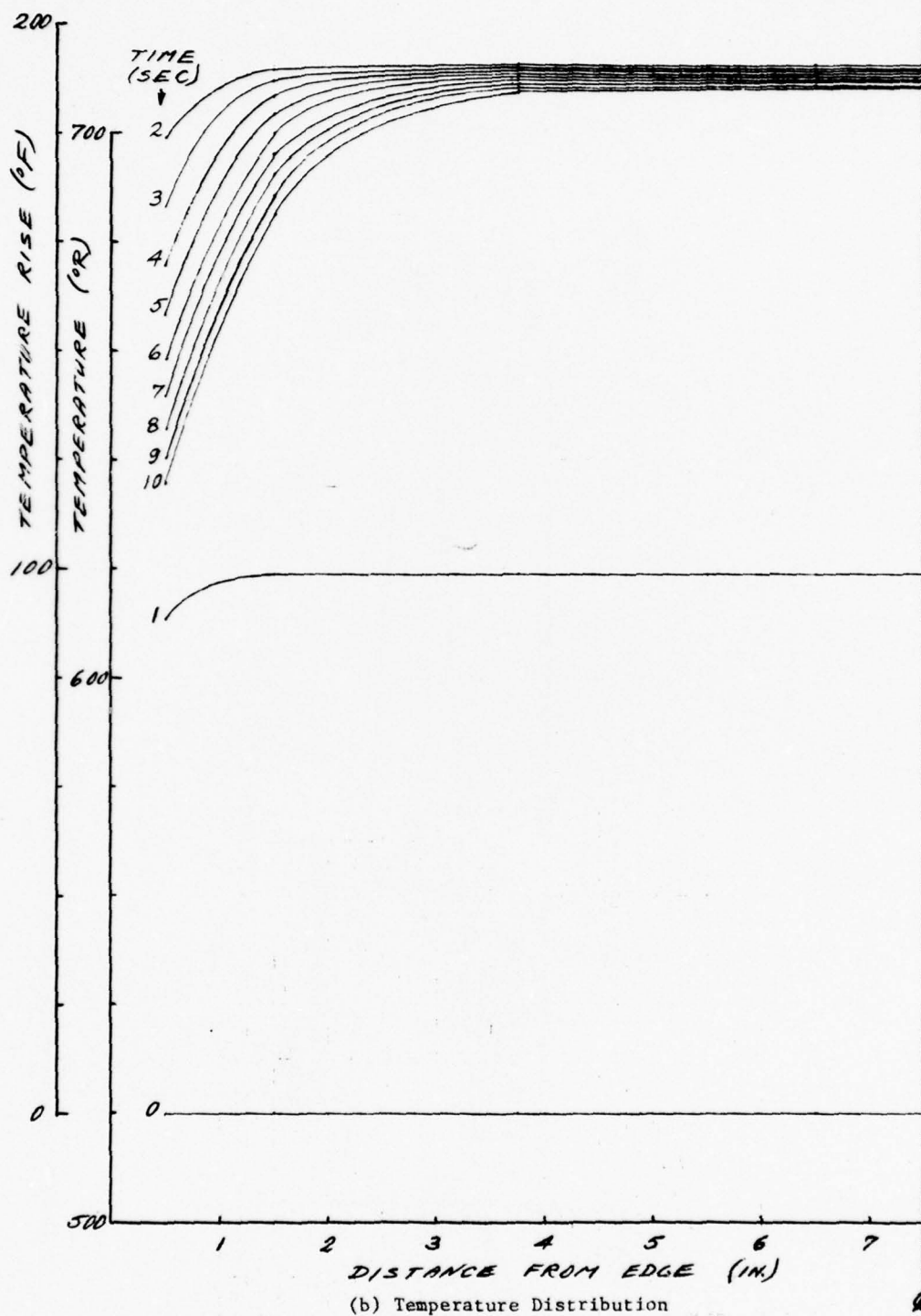
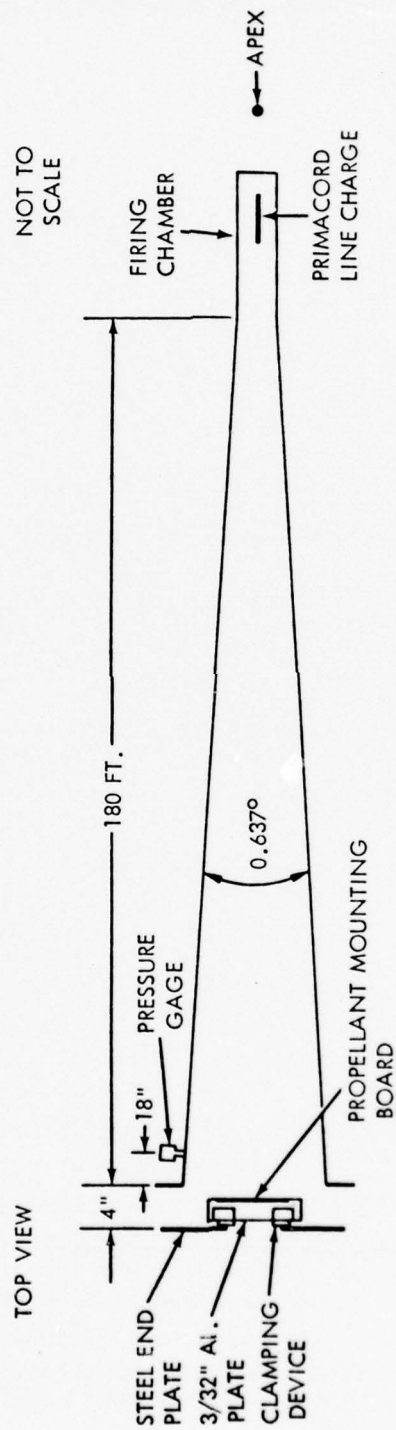
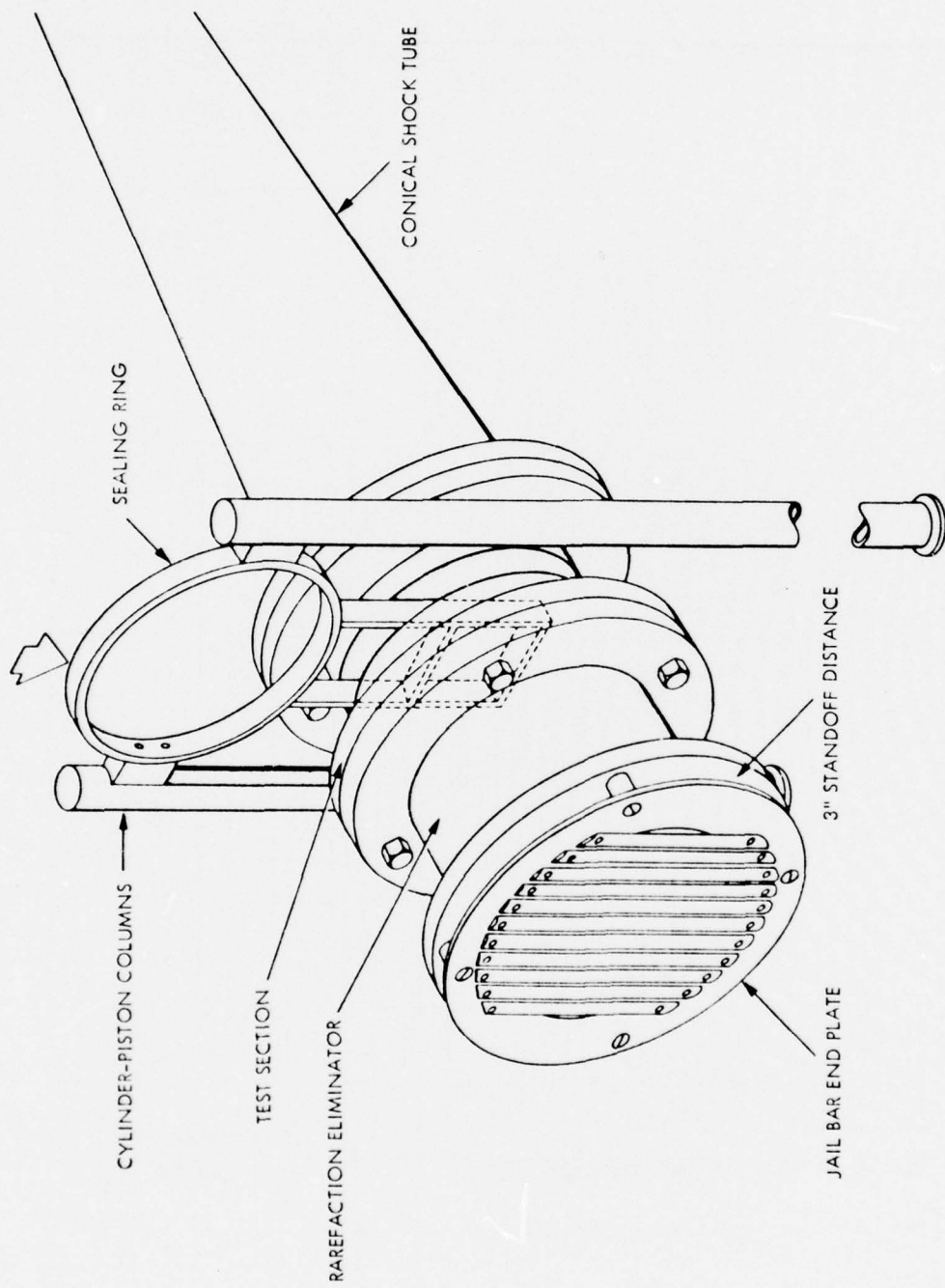


FIGURE 8. TEMPERATURE HISTORY AND DISTRIBUTION AT CENTERLINE OF SQUARE PANELS
SUBJECTED TO THERMAL EXPOSURE WITH A LARGE HEAT SINK AT EDGE



(a) Schematic of Shock Tube

FIGURE 9. THE NSWC EXPLOSIVELY DRIVEN CONICAL SHOCK TUBE WITH THERMAL EXPOSURE PROVISION



(b) Shock Tube Test Section Detail
 FIGURE 9. THE NSWC EXPLOSIVELY DRIVEN CONICAL SHOCK TUBE WITH THERMAL EXPOSURE PROVISION

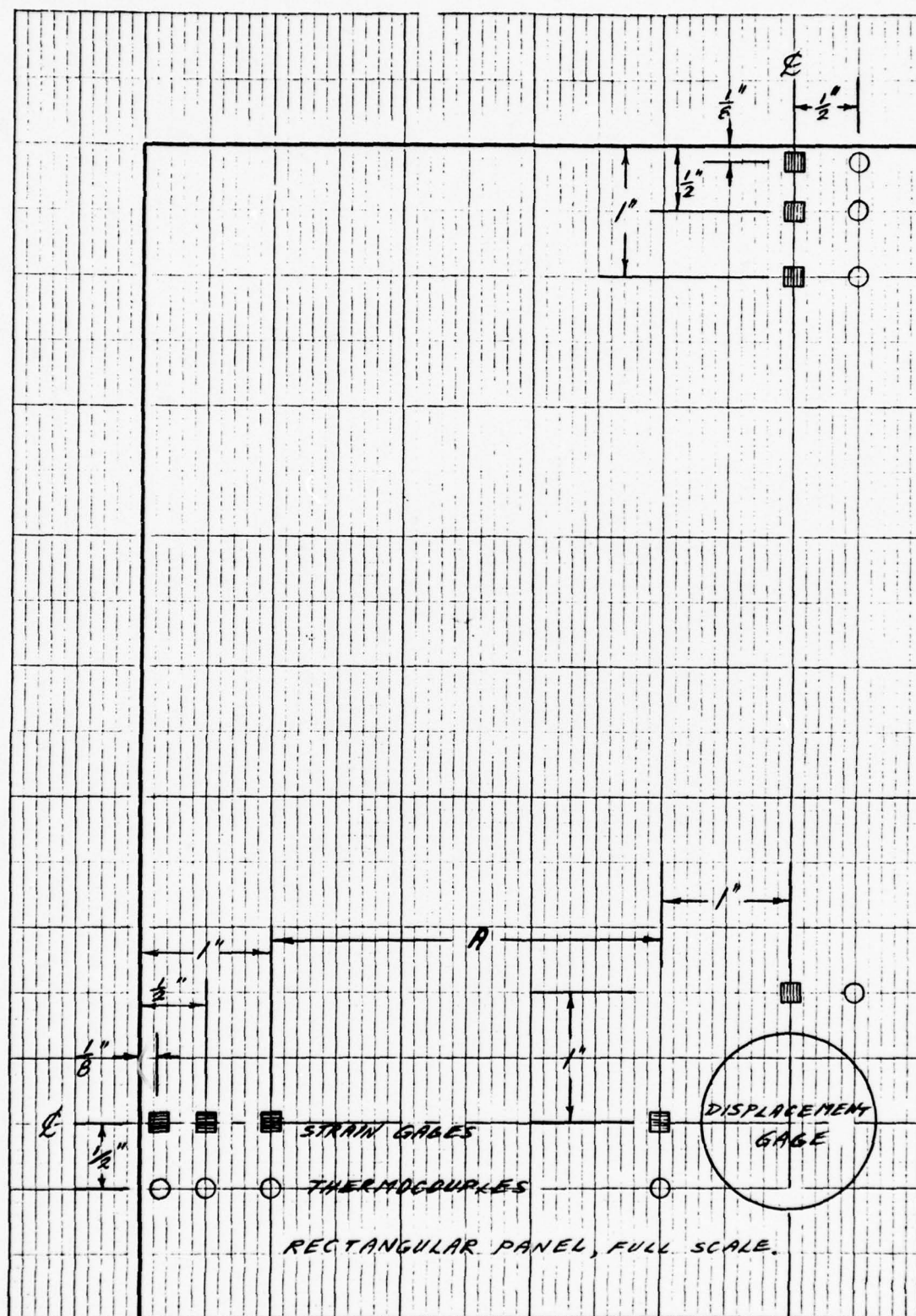


FIGURE 10. STRAIN GAGE AND THERMOCOUPLE LOCATIONS ON INNER SURFACE FOR THERMAL EXPOSURE CASES

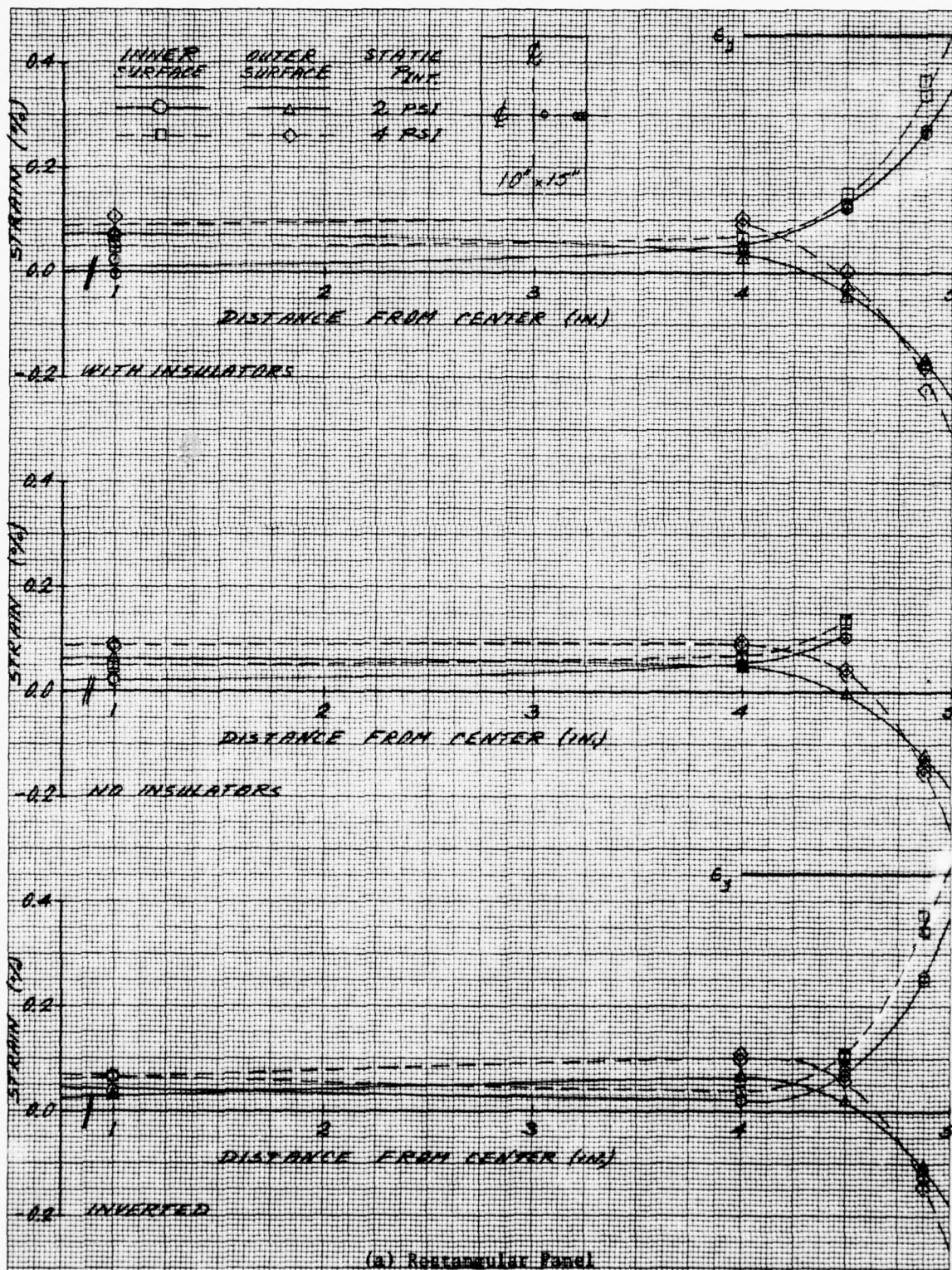
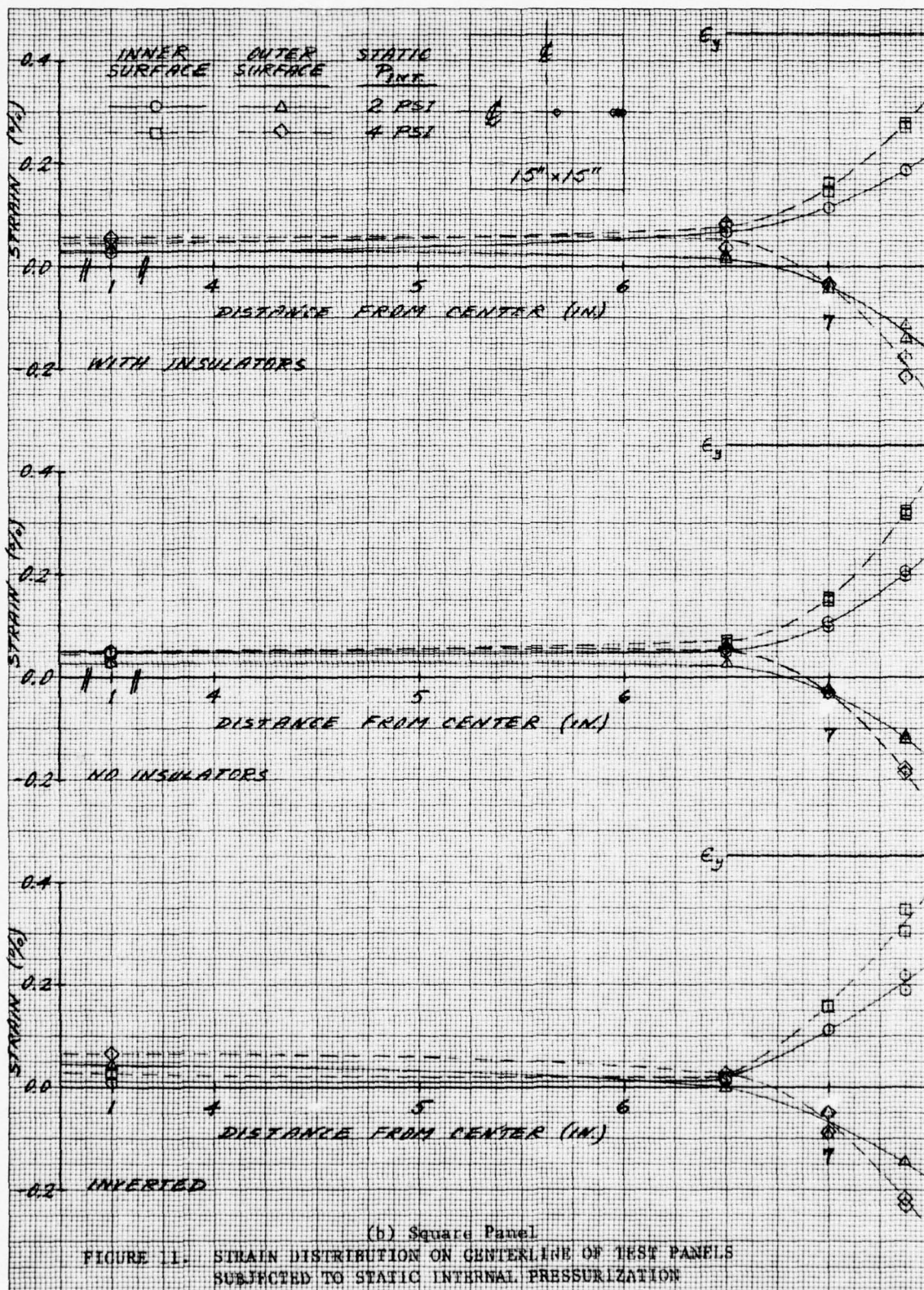


FIGURE 11. STRAIN DISTRIBUTION ON CENTERLINE OF TEST PANELS SUBJECTED TO STATIC INTERNAL PRESSURIZATION



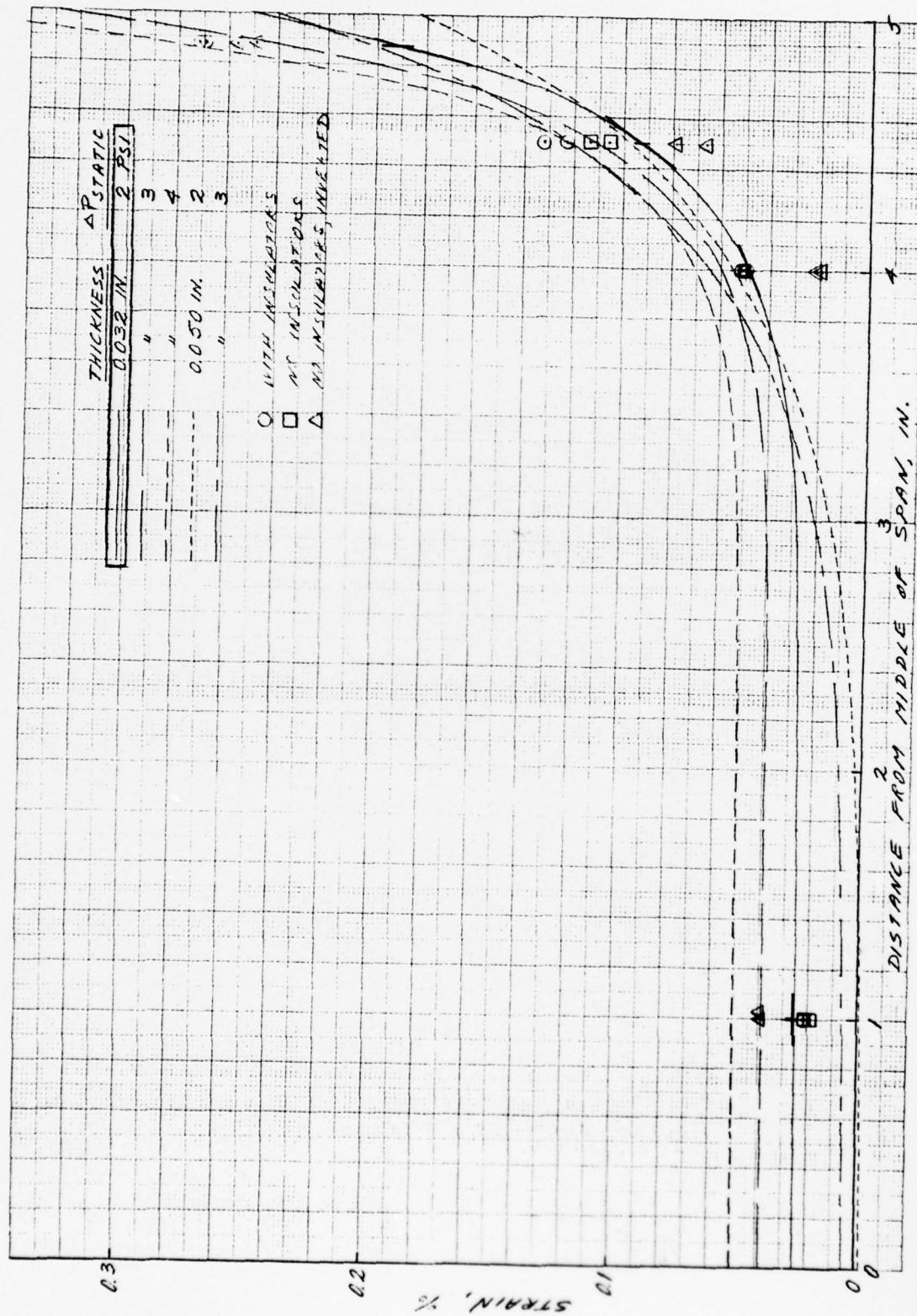
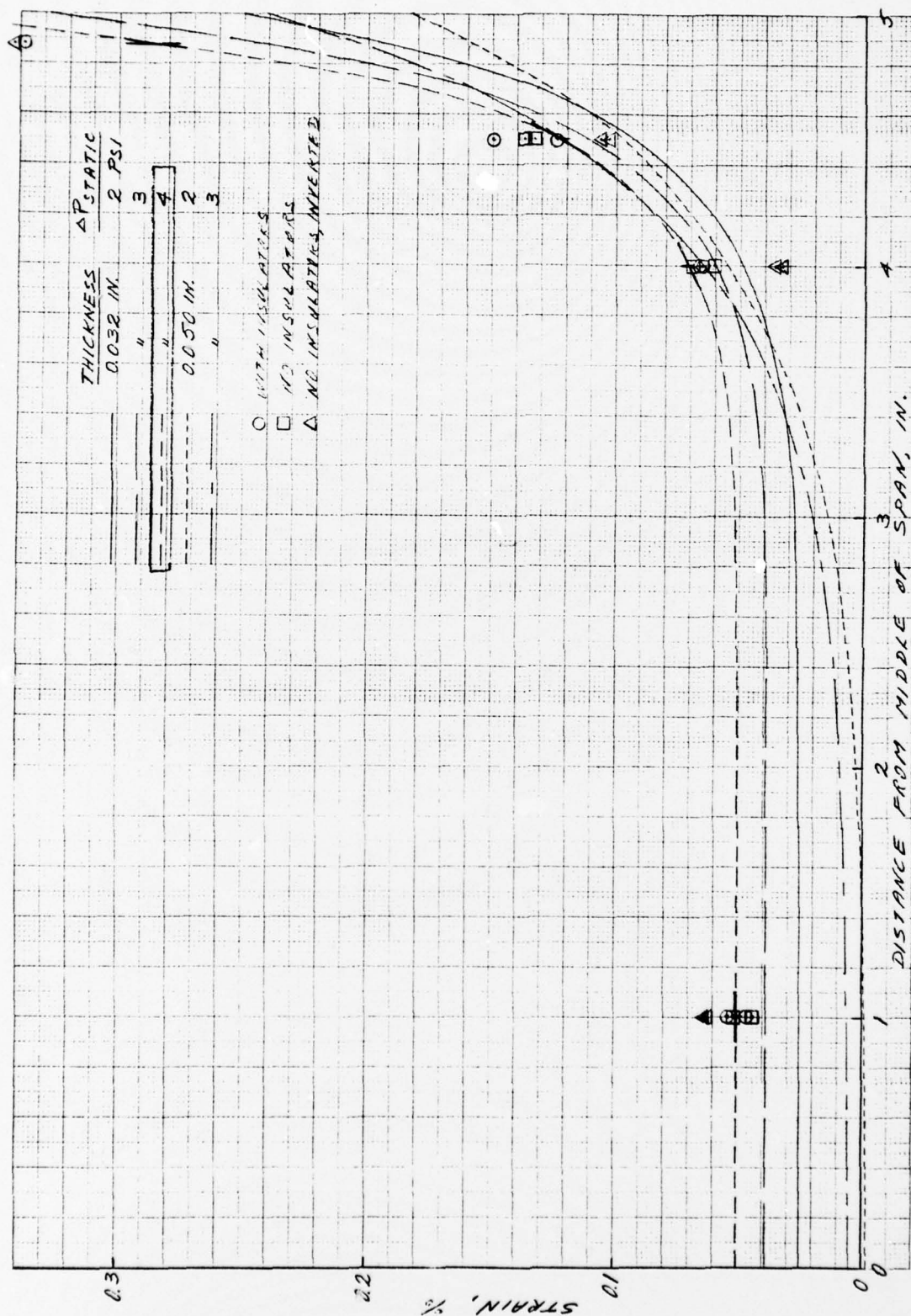


FIGURE 12. STRAIN DATA IN COMPARISON WITH ANALYTICAL RESULTS FOR RECTANGULAR PANELS SUBJECTED STATIC INTERNAL PRESSURIZATION

(a) $P_i = 2.0$ psi



(b) $P_i = 4.0$ psi

FIGURE 12. STRAIN DATA IN COMPARISON WITH ANALYTICAL RESULTS FOR RECTANGULAR PANELS SUBJECTED INTERNAL PRESSURIZATION

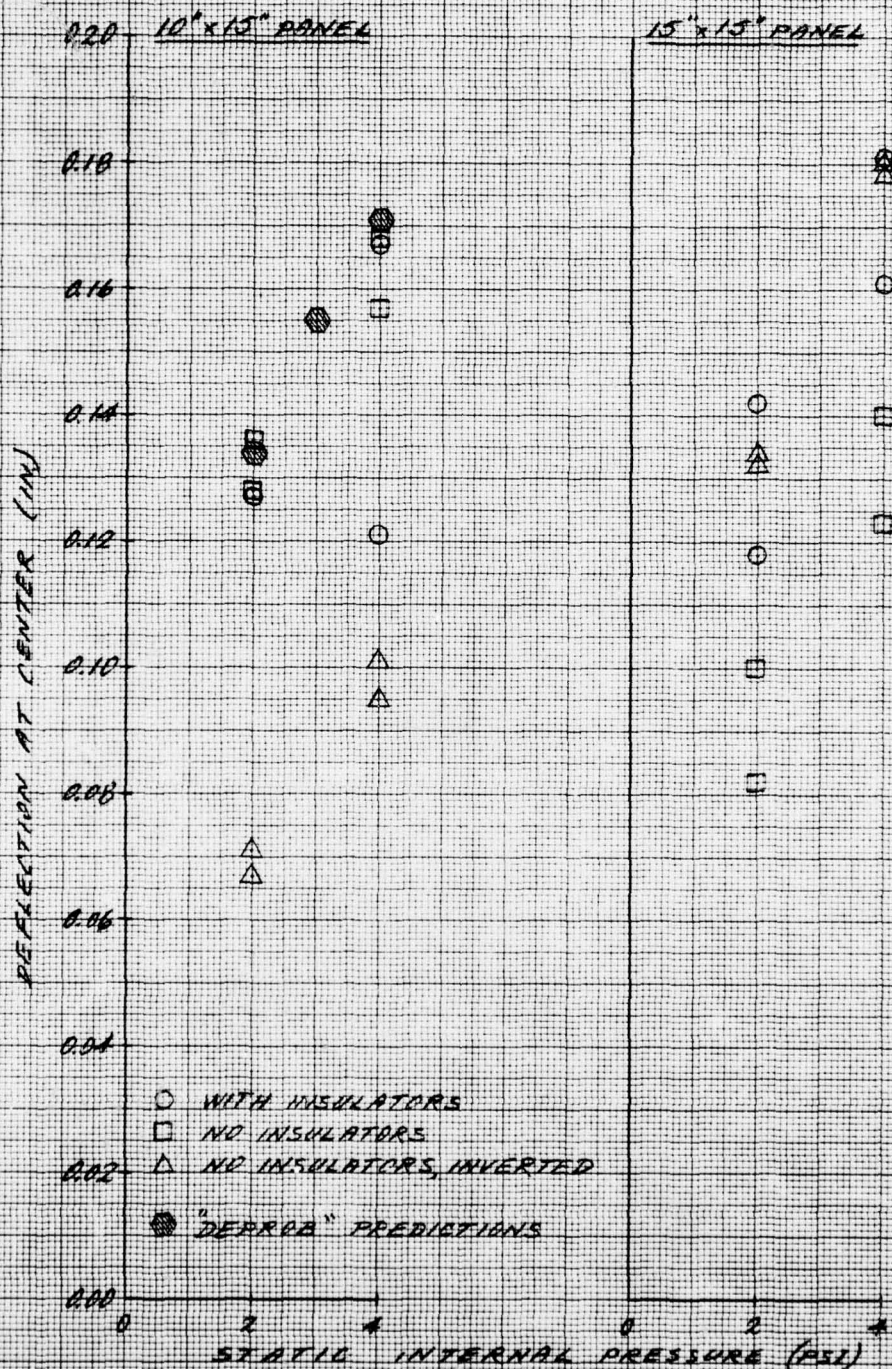


FIGURE 13. DEFLECTIONS AT CENTER OF PANELS SUBJECTED TO STATIC INTERNAL PRESSURIZATION

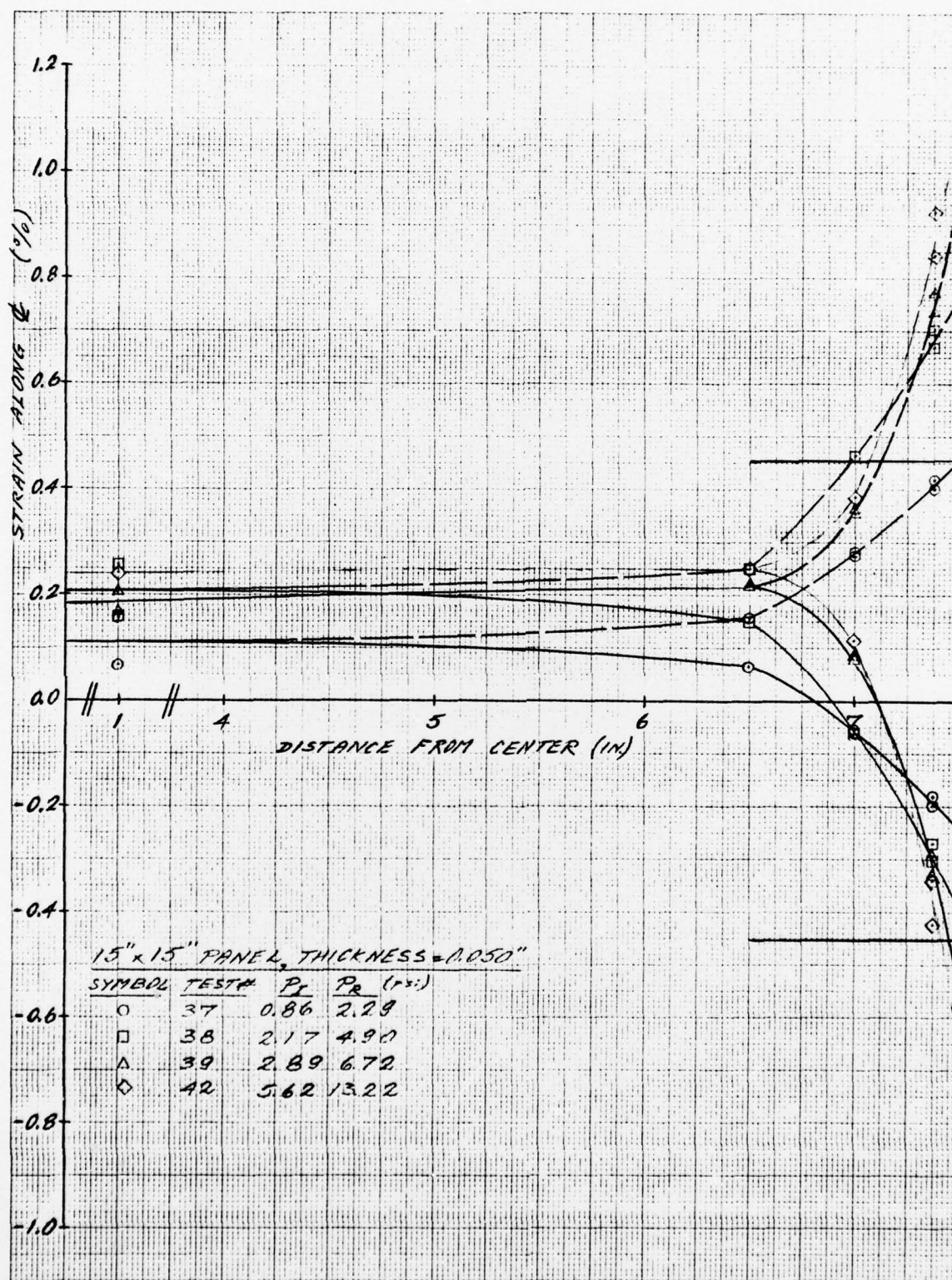


FIGURE 14. STRAIN DISTRIBUTION ON CENTERLINE OF SQUARE PANELS SUBJECTED TO BLAST OVERPRESSURE

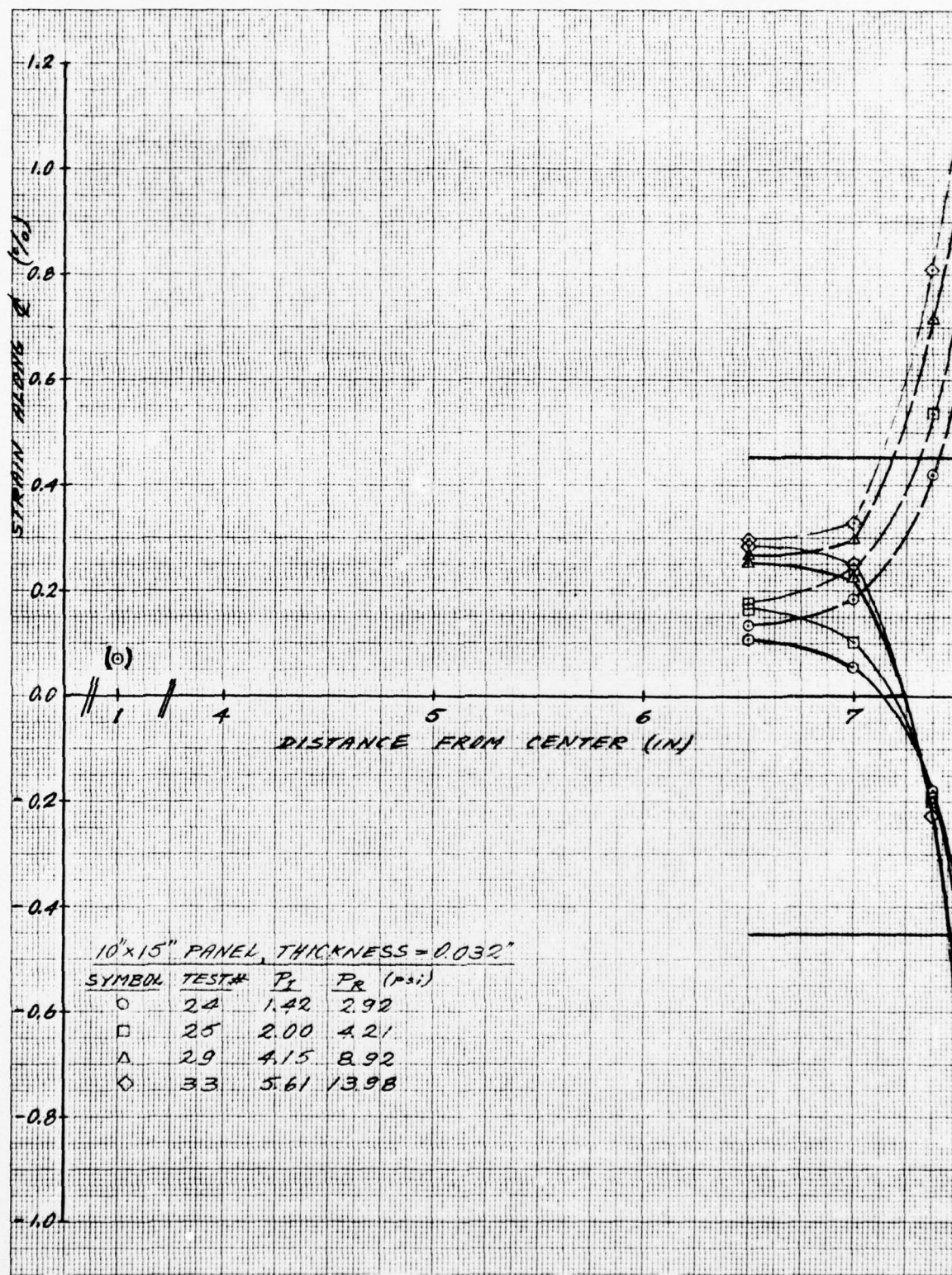


FIGURE 15. STRAIN DISTRIBUTION ON LONGER CENTERLINE OF RECTANGULAR PANELS
SUBJECTED TO BLAST OVERPRESSURE

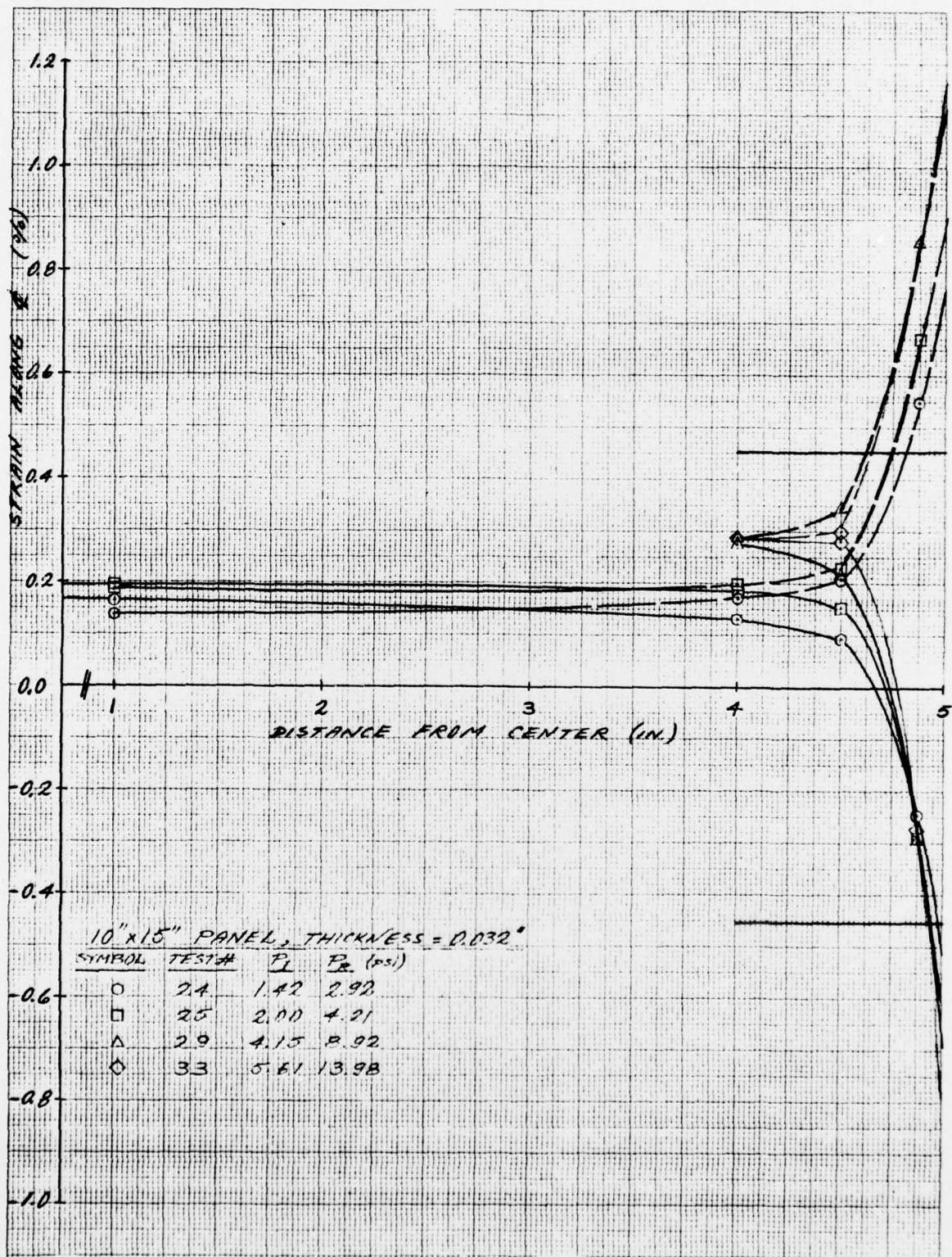


FIGURE 16. STRAIN DISTRIBUTION ON SHORTER CENTERLINE OF RECTANGULAR PANELS
SUBJECTED TO BLAST OVERPRESSURE

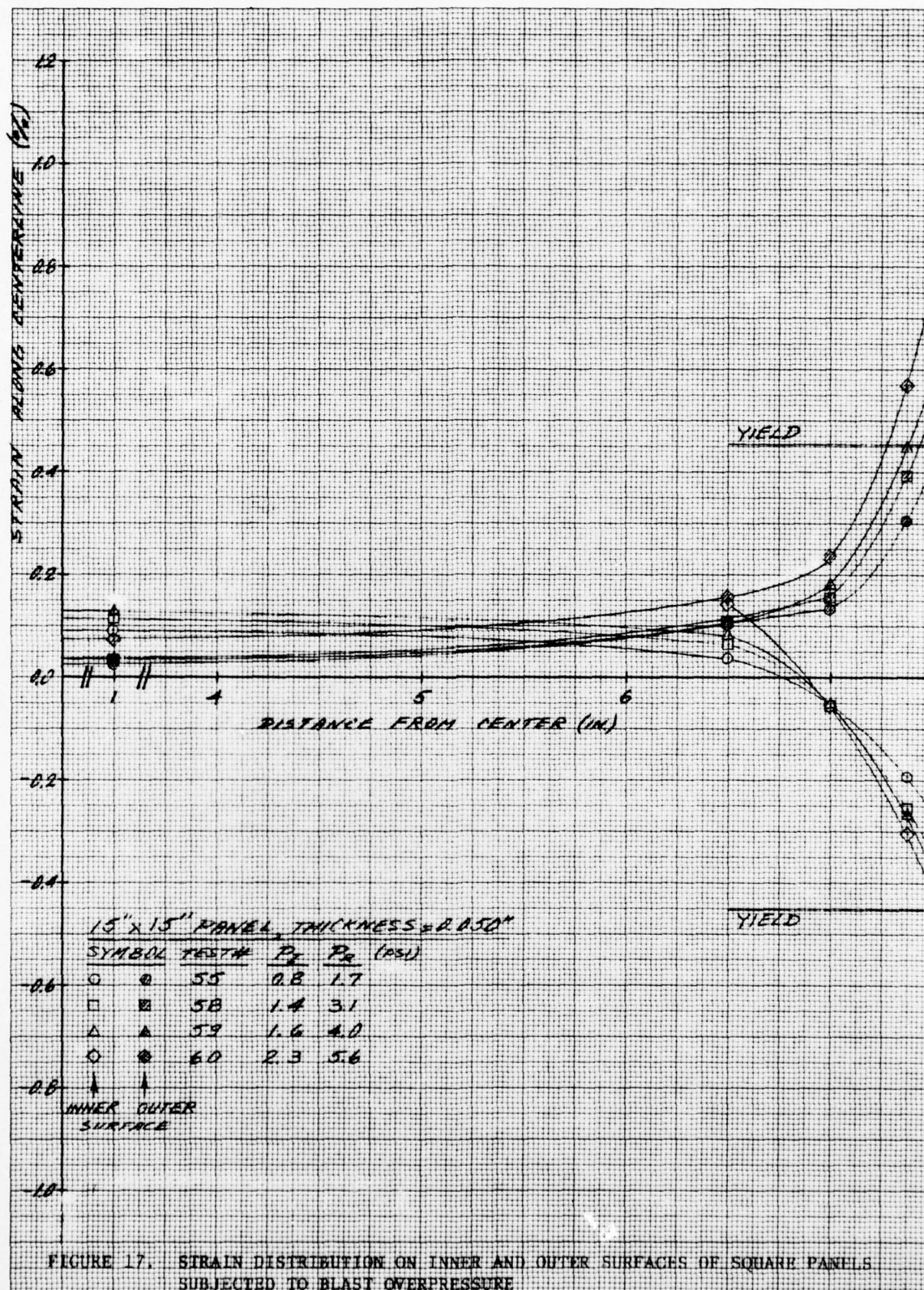


FIGURE 17. STRAIN DISTRIBUTION ON INNER AND OUTER SURFACES OF SQUARE PANELS SUBJECTED TO BLAST OVERPRESSURE

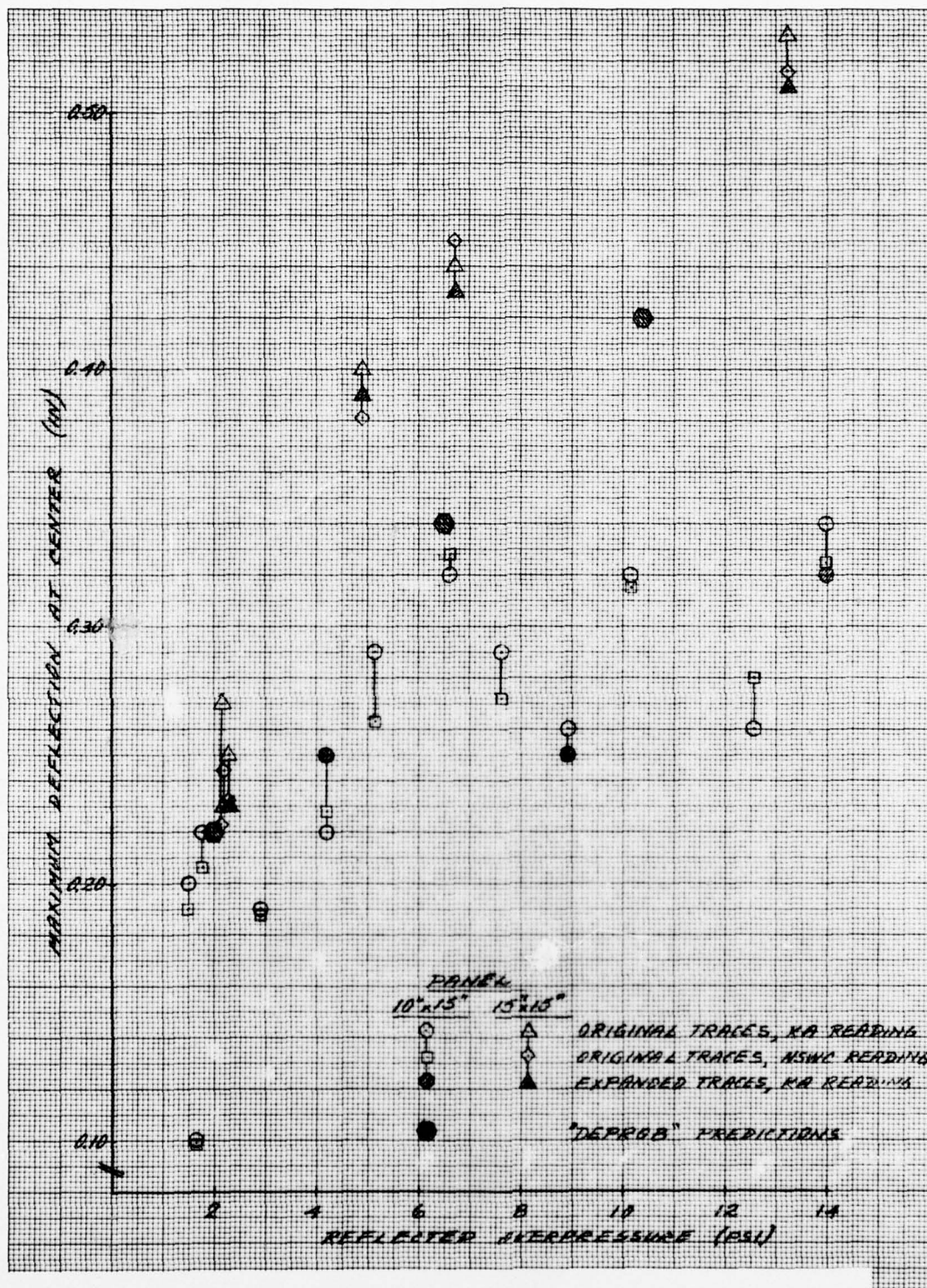


FIGURE 18. MAXIMUM DEFLECTION AT CENTER OF PANELS
SUBJECTED TO BLAST OVERPRESSURE

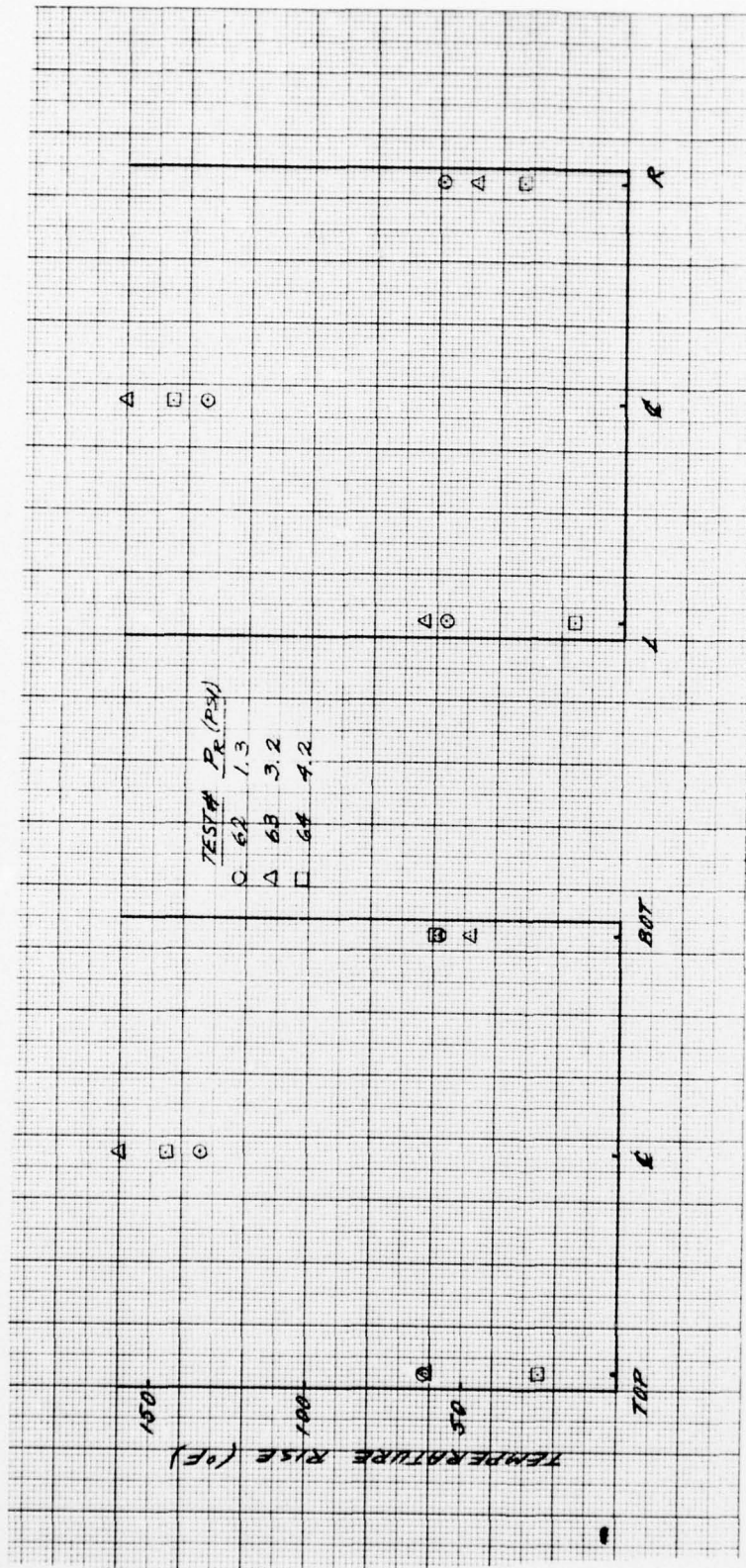


FIGURE 19. (a) 150° Target Temperature Rise
TEMPERATURE DISTRIBUTION ON BOTH CENTERLINES OF SQUARE PANELS SUBJECTED TO THERMAL
EXPOSURE PRIOR TO ARRIVAL OF BLAST OVERPRESSURE

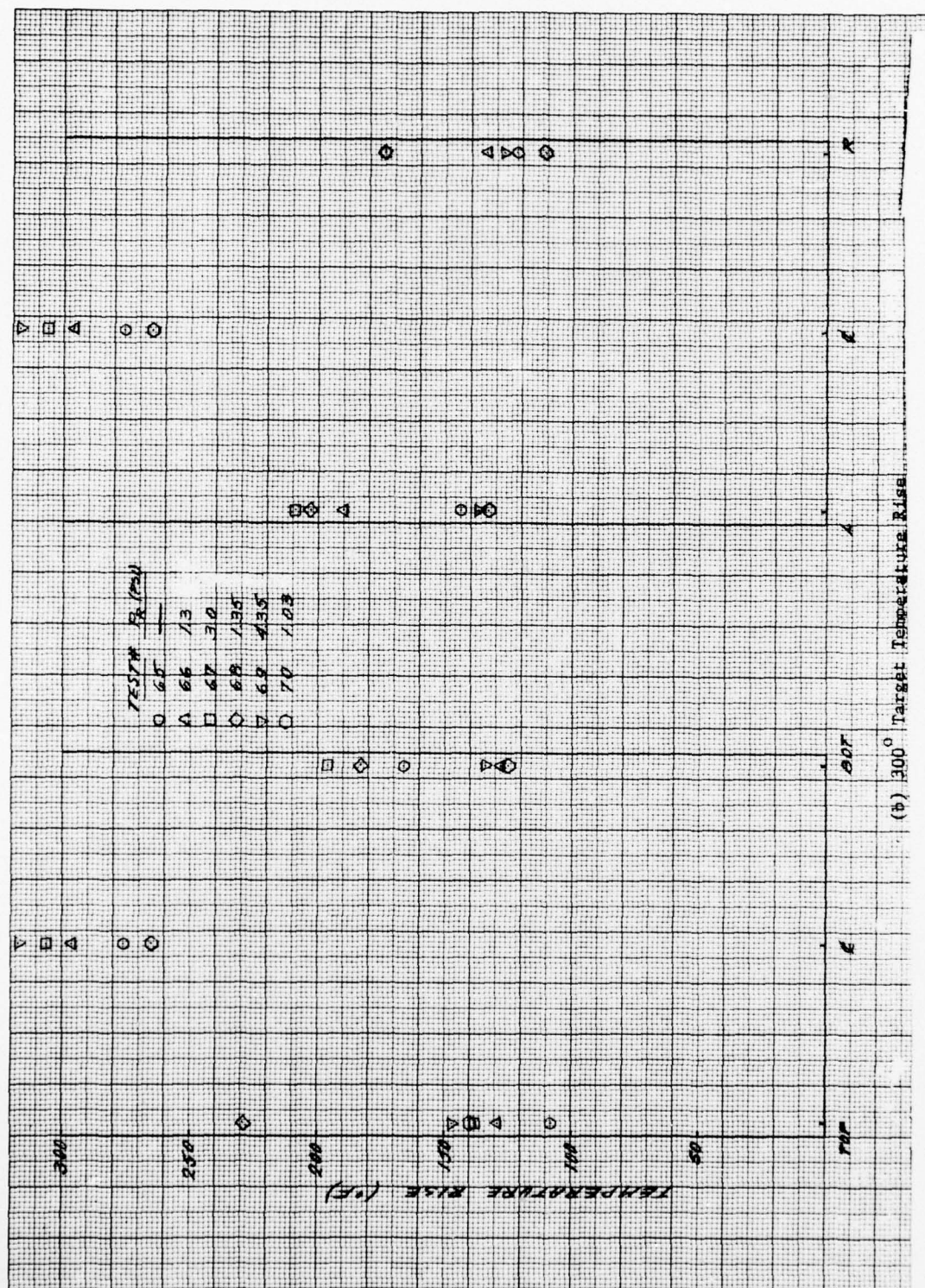
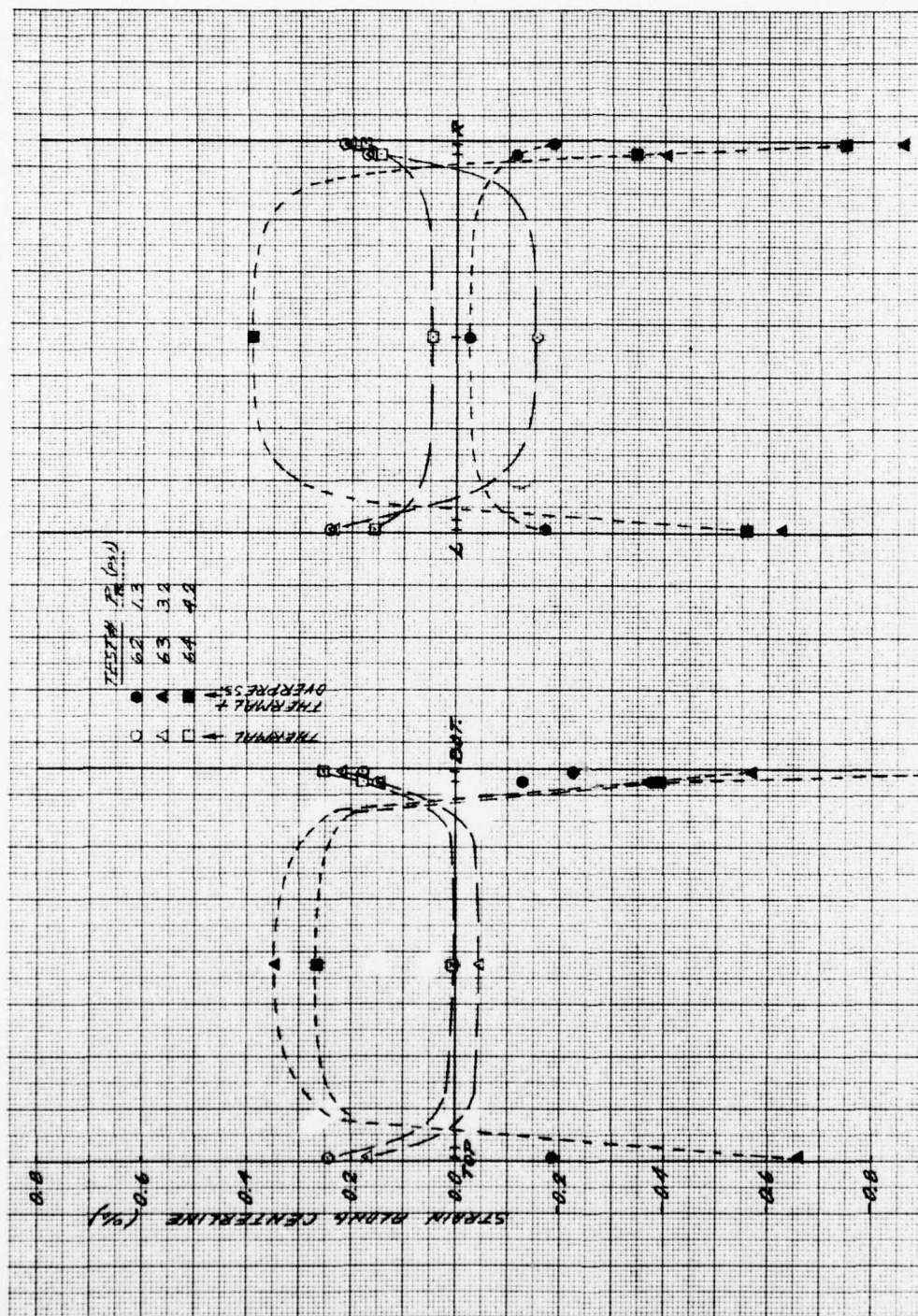


FIGURE 19. TEMPERATURE DISTRIBUTION ON BOTH CENTERLINES OF SQUARE PANELS SUBJECTED TO THERMAL EXPOSURE PRIOR TO ARRIVAL OF BLAST OVERPRESSURE



(a) 150° Target Temperature Rise

FIGURE 20. STRAIN DISTRIBUTION ON BOTH CENTERLINES OF SQUARE PANELS SUBJECTED TO COMBINED THERMAL/BLAST OVERPRESSURE EXPOSURE

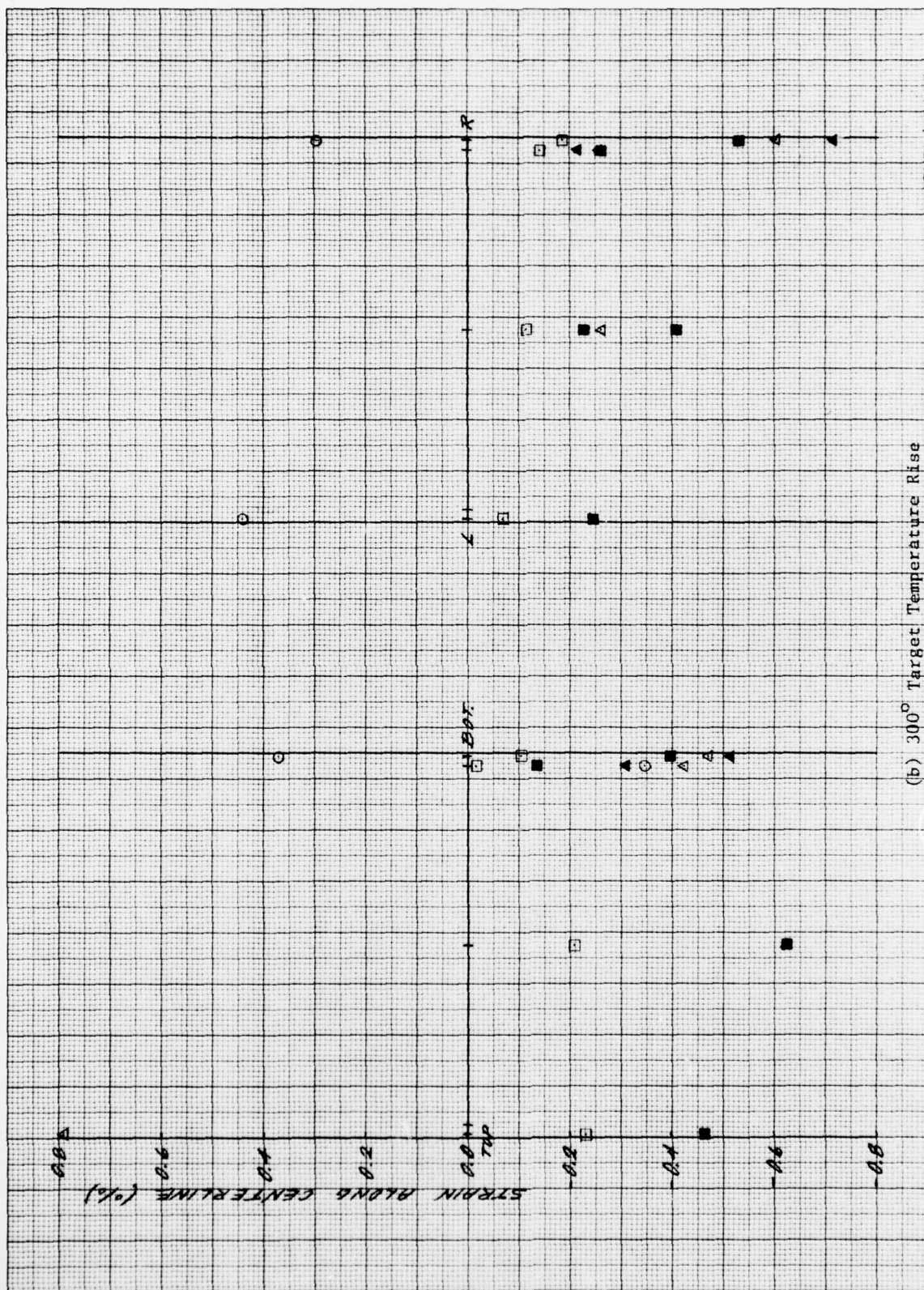


FIGURE 20. STRAIN DISTRIBUTION ON BOTH CENTERLINES OF SQUARE PANELS SUBJECTED TO COMBINED THERMAL/BLAST OVERPRESSURE EXPOSURE

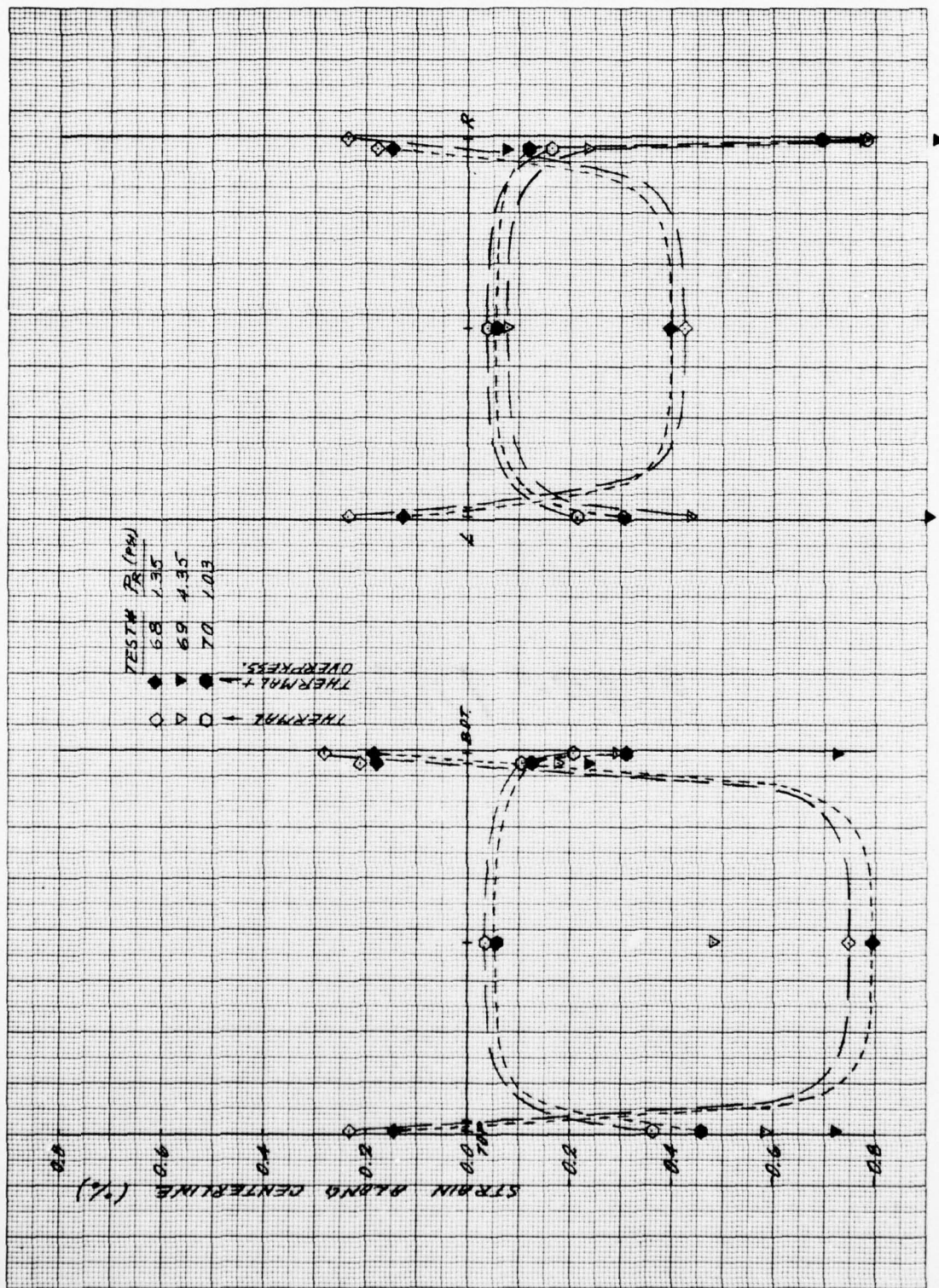


FIGURE 20. STRAIN DISTRIBUTION ON BOTH CENTERLINES OF SQUARE PANELS SUBJECTED TO COMBINED THERMAL/BLAST OVERPRESSURE EXPOSURE

(c) 300° Target Temperature Rise (concl.)

DISTRIBUTION LIST

DEPARTMENT OF DEFENSE

Director
Defense Nuclear Agency
ATTN: SPAS
ATTN: DDST
ATTN: STSP
ATTN: TISI Archives
3 cy ATTN: TITL Tech. Library

Under Sec'y of Def. for Rsch. & Engrg.
ATTN: S&SS (OS)

Commander
Field Command, Defense Nuclear Agency
ATTN: FCPR

Chief
Livermore Division, FCDNA
ATTN: FCPR

Defense Documentation Center
Cameron Station
12 cy ATTN: TC

DEPARTMENT OF THE ARMY

Commander
Harry Diamond Laboratories
ATTN: DRXDO-RBH, James H. Gwaltney
ATTN: DELHD-NP

Director
U.S. Army Ballistic Research Labs.
ATTN: DRXBR-X, Julius J. Meszaros

Commander
U.S. Army Materiel Dev. & Readiness Cmd.
ATTN: DRCDE-D, Lawrence Flynn

Commander
U.S. Army Nuclear Agency
ATTN: MAJ J. Vecke

DEPARTMENT OF THE NAVY

Chief of Naval Material
ATTN: MAT 0323

Chief of Naval Research
ATTN: Code 464, Thomas P. Quinn

Director
Naval Research Laboratory
ATTN: Code 2600, Tech. Lib.

Officer-in-Charge
Naval Surface Weapons Center
ATTN: Ken Caudle

Commanding Officer
Naval Weapons Evaluation Facility
ATTN: Peter Hughes

Director
Strategic Systems Project Office
ATTN: NSP-272

DEPARTMENT OF THE AIR FORCE

AF Materials Laboratory, AFSC
ATTN: MBC, Donald L. Schmidt
ATTN: MBE

AF Weapons Laboratory, AFSC
ATTN: DYV, Al Sharp
ATTN: SUL

Commander
ASD
4 cy ATTN: ENFTV, D. Ward

Commander
Foreign Technology Division, AFSC
ATTN: PDBF, Mr. Spring

Commander in Chief
Strategic Air Command
ATTN: XPFS

DEPARTMENT OF ENERGY

Sandia Laboratories
ATTN: Doc. Control for D. McCloskey

DEPARTMENT OF DEFENSE CONTRACTORS

Aerospace Corporation
ATTN: W. Barry

Avco Research & Systems Group
ATTN: J. Patrick
ATTN: William Broding

The Boeing Company
ATTN: Ed York
ATTN: Robert Dyrda

Boeing Wichita Company
ATTN: R. Syring
ATTN: D. Pierson

Effects Technology, Inc.
ATTN: Richard Parisse

General Dynamics Corp.
Fort Worth Division
ATTN: R. Shemensky

General Electric Company
TEMPO-Center for Advanced Studies
ATTN: DASAC

Kaman Avidyne
Division of Kaman Sciences Corp.
ATTN: Norman P. Hobbs
ATTN: Raffi P. Yeghiayan

Kaman Sciences Corporation
ATTN: Donald C. Sachs

Martin Marietta Corporation
Orlando Division
ATTN: Gene Aiello

DEPARTMENT OF DEFENSE CONTRACTORS (Continued)

McDonnell Douglas Corporation
ATTN: J. McGrew

Northrop Corporation
ATTN: Don Hicks

Prototype Development Associates, Inc.
ATTN: John McDonald

R&D Associates
ATTN: Jerry Carpenter
ATTN: F. A. Field
ATTN: Albert L. Latter

DEPARTMENT OF DEFENSE CONTRACTORS (Continued)

Rockwell International Corporation
ATTN: R. Sparling

Science Applications, Inc.
ATTN: Dwane Hove

SRI International
ATTN: George R. Abrahamson